UNIVERSITÀ DEGLI STUDI DI TRIESTE

XXIX CICLO DEL DOTTORATO DI RICERCA IN NANOTECNOLOGIE

Comprehension of the mechanisms that govern the potential adverse effects of nanomaterials on biological systems

Settore scientifico-disciplinare: Area 09 – Ingegneria industriale e dell'informazione
ING-IND/24 PRINCIPI DI INGEGNERIA CHIMICA

DOTTORANDO

Luca Viale

COORDINATORE

PROF. Lucia Pasquato

CO-SUPERVISORE

PROF. Sabrina Pricl

SUPERVISORE DI TESI

PROF. Anna L. Costa

ANNO ACCADEMICO 2015/2016

UNIVERSITÀ DEGLI STUDI DI TRIESTE

XXIX CICLO DEL DOTTORATO DI RICERCA IN NANOTECNOLOGIE

Comprehension of the mechanisms that govern the potential adverse effects of nanomaterials on biological systems

Settore scientifico-disciplinare: Area 09 – Ingegneria industriale e dell'informazione
ING-IND/24 PRINCIPI DI INGEGNERIA CHIMICA

DOTTORANDO

Luca Viale

COORDINATORE

PROF. Lucia Pasquato

CO-SUPERVISORE

PROF. Sabrina Pricl

SUPERVISORE DI TESI

PROF. Anna L. Costa

ANNO ACCADEMICO 2015/2016

Contents

1 INTRODUCTION

1.1 Nanomaterials ubiquity

Nanoparticles, defined by IUPAC as particles of any shape with at least one dimension in the 1×10^{-9} and 1×10^{-7} m range, are leading the current advances in nanotechnology. The first products that take advantage from these materials are already available on the market, both for industrial users (e.g., energy production and catalysis) and for consumers (e.g., cosmetics) [1].

Numerous companies offer nanoscale materials as commodities (e.g., PlasmaChem GmbH, Nanopartz Inc.), while large-scale monolayer graphene produced by roll-to-roll, metal–organic chemical vapor deposition (MOCVD) is now a reality (CIGIT). In the energy sector, nanotechnology is a key driver for lowering the price of solar cell production (e.g., Nanosolar) while display and lighting technologies are employing quantum size effects to control luminescence in next-generation conducting polymer and quantum-dot displays (e.g., Samsung, QDVision, Cambridge Display Technologies) [2]. A large number of biotech companies are exploiting nanomaterials for drug delivery or biolabeling (e.g., Starpharma) leading to better diagnostic procedure and therapies for many diseases [3] or continuous health monitoring and semi-automated treatment using small and cheap sensors and other implantable devices [4]. Such applications are sometimes called “nano-enabled” because they utilize a combination of technologies but include nanotechnology as a key component.

The rapid growth of nanotechnology industry and its ever-increasing applications will inevitably increase the concentration of nanomaterials in the environment, with potential human and environmental exposure as a consequence [5], [6]. The human body is exposed to NPs through four possible routes: inhalation of airborne NPs, ingestion of drinking water or food additives, dermal penetration by skin contact, and injection of engineered nanomaterials [7]. Regarding the environment, nanomaterials may potentially effect it in three possible ways: (i) direct effect on

microorganisms, invertebrates, fish and other organisms; (ii) interaction with contaminants that may change the bioavailability of toxic compounds and/or nutrients; and (iii) changes to non-living environmental structures [8].

1.2 Nanomaterials and adverse effects

1.2.1 Toxicology, Ecotoxicology and nanotechnologies

New materials and substances may present potential harmful effects on living organisms and on the environment. The toxicology as we know it studies these problems for pure chemical substances and, to do so, it includes many different fields of study: chemistry, biology, medicine. In order to extend the coverage of the risk assessment to the environment it is required to involve also ecology. When nanomaterials, in particular nanoparticles (NPs), are examined, it is necessary to link the ecotoxicological behaviour to the exceptional physical structure introduced by these materials. This wider study is done by nanotoxicology, which is why it is a multidisciplinary challenge [9].

The first task of nanotoxicology is to gain an exhaustive understanding of the structure-activity relationship focused on the adverse effects of nanomaterials, pointing out which physicochemical properties, such as (particles' size, shape, and surface charge), are responsible for the activity [10]. It is demanded to highlight the most appropriate measurement unit to use when dose-response relationships are expressed. Safety threshold levels and relative toxicity information for new, nanostructured materials will have to be related, for example, to the material specific surface area [11].

1.2.2 Risks of nanotechnology, solutions from nanotechnology

Nanotechnology has large potential benefits to a range of areas. Nanomaterials have the potential to improve the environment through the development of new solutions to environmental problems. For example, applications of nanomaterials to detect, prevent and remove pollutants [12], or using nanotechnology to design cleaner industrial processes and create environmentally friendly products [13].

The scientific community has also started to collect data on the ecotoxicity for some nanomaterials but there is a big knowledge gap between environmental risks assessment for traditional substances and for nanomaterials, because of the different behaviours of the latter in relation with the experimental medium involved, that deeply hinders this kind of assessments [14]. Human nanotoxicology, compared to environmental studies of nanomaterials, has the advantage of decades of toxicology studies on inhalable particles for a wide range of particles, including asbestos, coalmine dust, silica and suspended particulate matter (PM) into air pollution. Many standardised protocols are available to assess the hazards of substances released into the environment, but while these have been developed for standard chemicals they are not always appropriate for nanomaterials and may lead to confusing results. Adaptation of these protocols and development of new ones is required for nanomaterials to obtain good data sets in terms of relevance and experimental reproducibility. Moreover, new toxicity assessment must contemplate also the fate and the behaviour of the nanomaterials while these cross different media; a challenge since engineered nanomaterials in the environment may have unpredictable activities and it is difficult to detect them over the background when natural occurring particles are also present [15].

1.2.3 Nanomaterials fate, (eco)toxicological pathways

Nanoparticles sources are both natural (e.g., geological and meteorological phenomena, combustion processes, biological activity) or anthropogenic, further separated in voluntary and involuntary (e.g., wielding, tire-wear). All these sources may lead to environmental contamination. NPs crossing different environmental compartments, during their natural fate, may go through modifications of their physical properties (aggregation, size and shape) and chemical properties due to interactions with aqueous media and other environmental or biological substances (dissolution, coating).

When human toxicity is considered, the respiratory system has been observed as the most important entrance for NPs into the human body and the study efforts have

been limited to the NPs concentration and mobility in air (i.e. dustiness), while artificial lysosomal fluid (ALF) and Gamble's solution have been used to simulate natural biological fluids (lung fluids) to study inhaled NPs interactions [16], [17]. It should also be noted that nanoparticles can also be adsorbed after deposition on the olfactory epithelium and directly be translocated to the brain [18]. In these studies, the exposure level and toxicant concentration are expressed as number of NPs per m^3 in the inhaled air, instead of the traditional mass per m^3.

Extending the issue towards other species requires to study different pathways such as dermal or digestive ones for mammals, but such routes need a better evaluation because data in the literature result scarce and contradictory, often focused only on certain types of NPs (e.g., TiO_2) [19]. The need of a more ethical use of animals caused to prefer in-vitro experiments for widespread toxicity screening. NPs are prone to alter their external properties in cell test media, by reacting with it or by changing the colloidal stability parameters. In order to avoid distorted results, DLVO theory parameters have to be carefully assessed to assist the interpretation of the outcomes [18]. Such studies can be used to establish concentration–effect relationships and the effect-specific thresholds in cells. These assays are suited for high-throughput screening of an ever-increasing number of new engineered nanomaterials obviating the need for in-vivo testing of individual materials. They also serve as well-defined systems for studying the structure–activity relationships involving nanomaterials [20].

Ecotoxicological evaluation comprehends many different biological compartment and forces to study other characteristics of nanomaterials such as the environmental chemistry. These studies highlighted many knowledge gaps and key challenges to be solved before being able to achieve a comprehensive risk assessment and provide monitoring tools [14].

1.2.4 DLVO Theory

Nanoparticles dispersed in a liquid medium display the distinctive properties of colloidal systems, where constant Brownian movement of particles counter balance

the gravitational force and no separation of phases occurs. The stability of nanoparticles colloidal suspensions is improved by many factors such as diluted systems, small particles diameter, low density of the material. The achieved kinetic stability of the suspension ensures that it remains dispersed within the duration of experiment, without reaching the thermodynamic equilibrium and phase separation. The interparticle forces govern the settling rate by promoting agglomeration, that drifts the system towards phase separation, or aiding the colloidal stability through repulsion. The DLVO theory identifies three main categories of interaction forces: electrostatic, steric and van der Waals.

Electrostatic interaction occurs at the electric double layer of the charged particles; in this region, a charge separation occurs due to the interaction between the particle surface and the medium (water with dissolved species). The overall system is electrically neutral at all times, but the particles surface may have a charge. To balance this charge, an opposite charged layer constituted by oriented molecule and ions occurs in the solution, forming an electrical double layer with the particle surface. The electrostatic interaction between different particles is screened by the electrolytes in the solution and becomes relevant only when two surfaces approach each other at very short distances, typically of few nanometres. This interaction is attractive for different charges and repulsive when the charges are of the same sign, if the particles in solution are of the same material the force is always repulsive.

Steric interaction occurs between surfaces coated by long molecules (e.g., surfactants, polymers, proteins) as a consequence of the tail-tail interaction: there is an energetic cost to arrange molecules near each other, and overlap their electron clouds, due to a local diminution of entropy. This interference, when occurs, leads always to repulsion.

The third type of interaction comes from the Van der Waals forces, that are always present at short range and always attractive even if with low energies involved. In Figure 1.1 is reported an example of the energy curve in function of distance (H), derived from the summation of attractive (V_A) and repulsive (V_R) contributions, that

form the basis of the theory of colloid stability as stated by Deryaguin, Landauand, Verwey and Overbeek (DLVO theory).

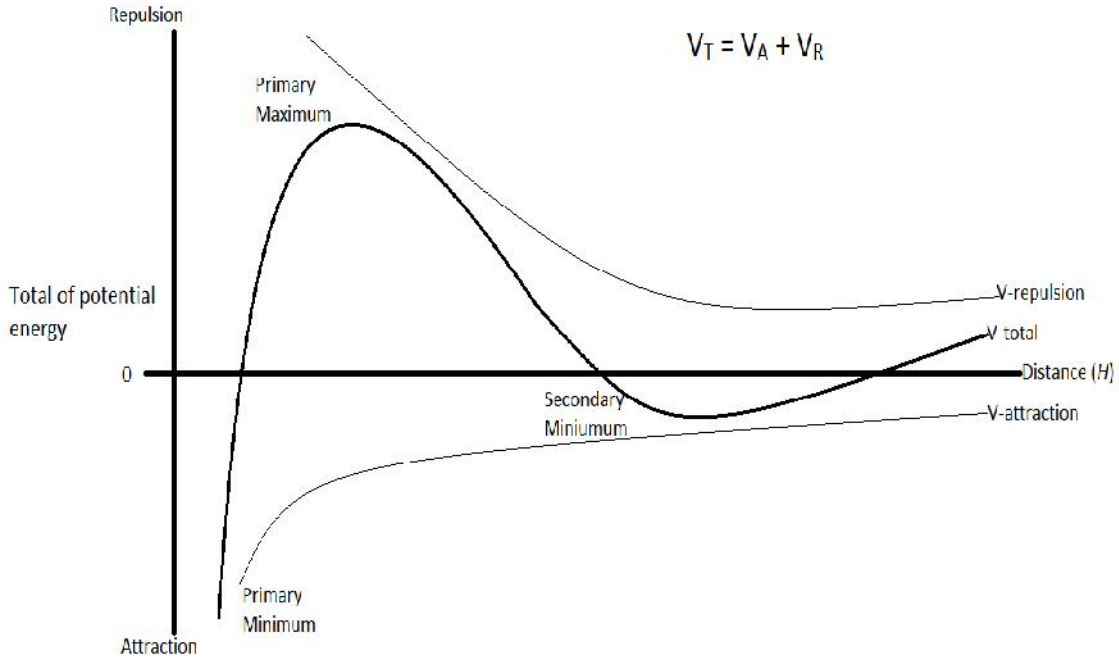

Figure 1.1 Energy potential vs interparticle interaction: DLVO theory

It can be noted that the system presents two regions of aggregation, corresponding to primary minimum and secondary minimum, separated by a repulsive barrier that gives raise to the primary maximum. When repulsive forces prevail, the colloidal suspensions are stable and sediment under gravity only after a long time, even years, to form a close-packed sediment. When attractive forces prevail various types of agglomerated structures may be formed, depending on the nature of the system and the forces involved. If the energy balance brings the particles in the primary minimum, strong attraction, coagulation occurs; the particles bound to each other and form a continuous particle network at high solid concentration, or in most cases, reach dimensions high enough to undergo a fast sedimentation. The case where attractive forces are balanced by the repulsive, driving the particle-particle distance in the secondary minimum, is referred to as flocculation: the particles are only weakly agglomerated, forming kinetic units in which the original particle volume is still distinguished. This is the case of reversible flocculation-deflocculation, where the suspension, driven by weak forces, forms a gel that can be broken by mechanical

agitation (e.g., ultrasonic mixing). The balance between attractive and repulsive forces is therefore the main factor that affects the stability of the colloidal suspensions and, in the case of nanosols, the possibility to preserve and show nanoscale reactivity. In order to predict the agglomeration state of suspensions and evaluate stability or manipulate the properties, it is necessary to collect as much information as possible about nanostructure and the nature of interparticle forces in water or biologically relevant media. Different techniques can be applied to evaluate particle size distribution (PSD) of colloidal systems. The state of agglomeration can be estimated by comparing primary structure size (XRD crystallite, TEM, BET equivalent) with that of secondary structure measured directly into wet medium (Dynamic Light Scattering, DLS; Laser Diffraction Analysis, LDA; Ultrasonic Attenuation Technique, UAS).

The U.S. National Institute of Standards and Technology (NIST) defined the average agglomeration number (AAN) as an estimation of the degree of agglomeration in a suspension. AAN is the average number of primary particles contained within an agglomerate. AAN is calculated as the ratio of the median particle size, as determined by light scattering techniques, and the average equivalent spherical volume (V), calculated from the BET gas adsorption method:

$$AAN = \frac{V_{50}}{V_{BET}} = \left(\frac{D_{50} \cdot SSA \cdot \rho}{6} \right)^3$$

where V_{50} is the equivalent spherical volume calculated from the median diameter (m^3), D_{50} is the size that splits the distribution with half above and half below this diameter (m), SSA is the specific surface area (m^2g^{-1}), ρ is the particle density (g m^3) and 6 is set as a spherical approximation factor [21].

1.3 Metal oxide nanoparticles

Presently, the group of the most important nanomaterials, for the worldwide market, includes simple metal oxides such as titanium dioxide (TiO_2), zinc oxide (ZnO), magnesium oxide (MgO), copper oxide (CuO), aluminium oxide (Al_2O_3), manganese oxide (MnO_2) and iron oxide (Fe_3O_4, Fe_2O_3). Metal and metal oxides NPs applications are growing in a wide range of fields; in 2015, such particles could be found in 37% of products listed in the Nanotechnology Consumer Product Inventory [22]. These materials are used as pigments in paints (TiO_2), as sunscreens and cosmetics additives (TiO_2, ZnO), as antimicrobial agents (MgO, CuO), as part of tools in industrial processes (Al_2O_3, MnO_2) and for medical purposes like as drug delivery systems, by encapsulating the drugs to increase dispersibility for evading clearance mechanisms and allowing the site-specific targeting of drugs to cells (Al_2O_3, Fe_3O_4, Fe_2O_3) [23], [24], [25], [26], [27], [28], [29].

Previous toxicological studies were conducted on Al_2O_3, TiO_2, CdO_2, ZnO, CuO, Fe_2O_3, Fe_3O_4 [23], [30], [31], [32].

1.3.1 Copper oxide nanoparticles

Copper oxide nanoparticles occurs naturally, for example volcanic eruption and fumaroles may lead to the formation of volcanic sublimate, including tenorite that is monoclinic CuO [48], and have been therefore present in the environment for thousands of years. In recent times, other anthropological sources have arisen, unintentionally releasing more copper nanoparticles; for example, municipal incinerators by-products or electrical related facility emission like power stations, electric bus, rail transports and subways [31], [49]. Today, the production of synthetic NPs as technological ingredients for a large selection of commercial products sums to the total exposure of CuO NPs in the environment and to humans, becoming major concern since the global market demands is estimated to increase in the next few years. Therefore, there is a considerable need to evaluate the exact toxic effects of CuO NPs associated with their usage in a variety of applications. The initial investigations showed that copper oxide nanoparticles are highly toxic, even more

than free Cu ions, as they may serve as “Trojan-horse type carriers” enabling the transport of metal ions into the cells [33]. Exposure to these particles, both occupationally or via consumer products, may pose a health risk.

Recently this material has attracted more attention due to its unique properties: as transition metal oxide, it exhibits a narrow band gap that forms the basis of several high temperature superconductors, gas sensors, giant magneto resistance materials, solar energy transformation and preparation of organic–inorganic nanostructure composites [34]. Applications include as an anti-microbial, anti-fouling, anti-biotic and anti-fungal agent when incorporated in coatings, plastics and textiles [35], [36]. The literature on CuO NPs synthesis and engineering has begun to consider this material later than other metal oxides and the reports on the preparation and characterization of nanocrystalline CuO are relatively scarce [37], [38]. Some of the methods reported so far include the sono-chemical method [39], sol–gel [40], one-step solid state reaction at room temperature [41], electrochemical [42], thermal decomposition of precursors [43], [44] and co-implantation of metal and oxygen ions [45], but there are also green synthesis procedures mediated by penicillium [46] and aloe barbadensis miller [34].

Nano CuO has been investigated as possible, economical, Ag NPs substitute in wound dressing [47]. As a further application, in recent years, nano CuO was investigated for preservative coating and as antifungal additive in paints [36].

1.4 Aim of the study

The aim of my PhD thesis is to face a commercial need: the necessity to use new technology without raising any safety concern in the stakeholders. To do so it is proposed a protocol for the introduction of “safety by molecular design” (SbyD) strategies. Such approach suggests to cut off every eco-toxicological issue, in a given commercial material, by re-thinking the production procedure and including in its design few modifications that will remove the HSE issues during all the product life cycle. The approach proposed in this work shows how to search for the best SbyD strategies by studying a commercial nanopowder that is also target of a European

research project: the European Sustainable Nanotechnologies project (SUN). It is consequently joined the European attempt provide environmental and health risks assessment for the given material and support their main goal to evaluate and develop technological alternatives and risk management measures (TARMM) considering the whole life cycle of nanomaterials, from manufacturing to disposal, in order to assist the successful development of nanotechnology (principles of sustainability).

1.4.1 European project Sustainable Nanotechnologies (SUN)

Unlike other nano-environmental, health and safety (HSE) projects advancing the understanding of the properties, interactions, fate, impacts and risks of nanomaterials, SUN project was envisioned to walk down the road from scientific implications to industrial applications while at the same time inform regulatory oversight. The SUN research process integrates the bottom-up generation of nano-HSE data and methods with the top-down design of a Decision Support System (DSS) for practical use by industries and regulators. The SUN industrial partners will test the DSS against supply chains of real products. This validation will culminate in guidelines for safe nanoscale product and process design [50].

Amongst SUN partners are included large and medium size enterprises together with private research centres, academics and public entities, that possess considerable experience in the field of NM occupational health and safety.

CNR-ISTEC, an Italian governmental organization for scientific research in the field of conventional, structural, bio and functional ceramic materials, coordinated the work package on Safe Production, Handling and Disposal of nanomaterials. Within this work package, industrial partners PlasmaChem and BASF provided the starting material and the nano-enabled commercial formulations (paints).

1.4.2 Safety by molecular design concept

Borrowed from the construction industry, the safety by design (SbyD) concept is an approach to innovation that focuses on the understanding of health and safety risks

before the beginning of the production. For nanotechnology and material design, this approach moves to the so-called molecular level: to reduce or design-out the risks throughout the entire life cycle of the new product, the specific issues have to be determined and managed together with product or process quality and efficiency, during early planning of the synthesis [51], [52], [53].

The NPs engineering following the SbyD concepts was highlighted as a strategic and priority area in the European Nanosafety Cluster and in the EU Nano-Safety Strategy 2015-2025 Agenda [54].

The safety by molecular design approach can be divided in a multi-step process as follows:

1. Preliminary dataset collection; involves the investigation of NPs physicochemical properties and toxicity, collecting the necessary information such as the mechanism that governed both the adverse effects on environment and biological systems (toxicity pathways) and the NPs exposure potential.
2. Modification of the product; contains changes to the initial design, to avoid concerns underlined in the first step, and experimental confirmation of the achieved modification.
3. Toxicological evaluation; here in-vitro and in-vivo tests are performed according to the relevant exposure pathways.
4. Implementation; a cost/benefit analysis of the new material performance and synthesis must be overtaken before the promotion of the SbyD strategy.

1.4.3 Surface engineering as SbyD strategy

The experience gained within the new research field of nanotoxicology suggests to identify the NPs property-activity relationships and build the mechanisms of risk remediation on these relationships. Although most materials are not yet fully understood, it is known that colloidal science properties regarding NPs influence their environmental and biological fate, consequently impacting on the uptake and

toxicity. These properties include NPs size, shape, surface chemistry and stability under some environmental and biological conditions [55].

There are already many different strategies for surface engineering development to control NPs toxicity and exposure, improving therefore their sustainability. For CuO NPs, that exercise its toxicity mechanism due to dissolution phenomena and ion leaching, surface engineering was exploited to modify the behaviour of the particles and potentially control ions release and bioavailability.

1.4.4 Specific objectives

In order to achieve the aim introduced in 1.4, I addressed the following specific objectives:

1) Development and sampling of pristine and SbyD modified samples.
2) Evaluation of physicochemical synthetic identity (structural and surface properties).
3) Evaluation of CuO exposure related physicochemical properties (colloidal properties in exposure relevant media).
4) Evaluation of CuO hazard related physicochemical properties (ions dissolution) and biological effects.
5) Performance evaluation for the justification of proposed solutions.

1.5 References

[1] P. V. Kamat, "Dominance of Metal Oxides in the Era of Nanotechnology," *The Journal of Physical Chemistry Letters,* vol. 2, no. 7, pp. 839-840, 2011.

[2] P. Mulvaney and P. S. Weiss, "Have Nanoscience and Nanotechnology Delivered?," *ACS Nano,* vol. 10, no. 8, pp. 7225-7226, 2016.

[3] A. G. Cuenca, H. Jiang, S. N. Hochwald, M. Delano, W. G. Cance and S. R. Grobmyer, "Emerging implications of nanotechnology on cancer diagnostics and therapeutics," *Cancer,* vol. 107, no. 3, pp. 459-466, 2006.

[4] M. C. Roco and W. S. Bainbridge, Overview Converging Technologies for Improving Human Performance, Dordrecht: Springer Netherlands, 2003, pp. 1-27.

[5] European Union, *Official Journal of the European Union, L 338,* 13 November 2004.

[6] Royal Society and the Royal Academy of Engineering, Nanoscience and nanotechnologies, London: Royal Society, 2004.

[7] G. Oberdörster, E. Oberdörster and J. Oberdörster, "Nanotoxicology: An Emerging Discipline Evolving from Studies of Ultrafine Particles," *Environmental Health Perspectives,* vol. 113, no. 7, pp. 823-839, 2005.

[8] J. R. Lead and E. L. Smith, Environmental and human health impacts of nanotechnology, Hoboken (NJ): Wiley, 2009.

[9] K. Donaldson, V. Stone, L. C. Tran, W. Kreyling and P. J. Borm, "Nanotoxicology," *Occupational and environmental medicine,* vol. 61, no. 9, pp. 727-728, 2004.

[10] H.-R. Paur, F. R. Cassee, J. Teeguarden, H. Fissan, S. Diabate, M. Aufderheide, W. G. Kreyling, O. Hänninen, G. Kasper, M. Riediker, B. Rothen-Rutishauser and O. Schmid, "In-vitro cell exposure studies for the assessment of nanoparticle toxicity in the lung—A dialog between aerosol science and biology," *Journal of Aerosol Science,* vol. 42, no. 10, pp. 668-692, 2011.

[11] K. Donaldson and C. A. Poland, "Nanotoxicity: challenging the myth of nano-specific toxicity," *Current Opinion in Biotechnology,* vol. 24, no. 4, pp. 724-734, 2013.

[12] P. V. Kamat and D. Meisel, "Nanoscience opportunities in environmental remediation," *Comptes Rendus Chimie,* vol. 6, no. 8-10, pp. 999-1007, 2003.

[13] A. Corma and H. Garcia, "Supported gold nanoparticles as catalysts for organic reactions," *Chemical Society Reviews,* vol. 37, no. 9, pp. 2096-2126, 2008.

[14] R. D. Handy, R. Owen and E. Valsami-Jones, “The ecotoxicology of nanoparticles and nanomaterials: current status, knowledge gaps, challenges, and future needs,” *Ecotoxicology,* vol. 17, no. 5, pp. 315-325, 2008.

[15] V. Stone, B. Nowack, A. Baun, N. van den Brink, F. von der Kammer, M. Dusinska, R. Handy, S. Hankin, M. Hassellöv, E. Joner and T. F. Fernandes, “Nanomaterials for environmental studies: Classification, reference material issues, and strategies for physico-chemical characterisation,” *Science of The Total Environment,* vol. 408, no. 7, pp. 1745-1754, 2010.

[16] P. H. Hoet, I. Brüske-Hohlfeld and O. V. Salata, “Nanoparticles – known and unknown health risks,” *Journal of Nanobiotechnology,* vol. 2, no. 12, 2004.

[17] W. S. Cho, R. Duffin, F. Thielbeer, M. Bradley, I. L. Megson, W. MacNee, C. A. Poland, C. L. Tran and K. Donaldson, “Zeta Potential and Solubility to Toxic Ions as Mechanisms of Lung Inflammation Caused by Metal/Metal Oxide Nanoparticles,” *Toxicological Sciences,* vol. 126, no. 2, pp. 469-477, 2012.

[18] J. Jiang, G. Oberdörster and P. Biswas, “Characterization of size, surface charge, and agglomeration state of nanoparticle dispersions for toxicological studies,” *Journal of Nanoparticle Research,* vol. 11, no. 1, pp. 77-89, 2008.

[19] M. Crosera, M. Bovenzi, G. Maina, G. Adami, C. Zanette, C. Florio and F. Filon Larese, “Nanoparticle dermal absorption and toxicity: a review of the literature,” *International Archives of Occupational and Environmental Health,* vol. 82, no. 9, pp. 1043-1055, 2009.

[20] S. Arora, J. M. Rajwade e K. M. Paknikar, «Nanotoxicology and in vitro studies: The need of the hour,» *Toxicology and Applied Pharmacology,* vol. 258, n. 2, pp. 151-165, 2012.

[21] V. A. Hackley, The use of nomenclature in dispersion science and technology, Gaithersburg, Md.: U.S. Dept. of Commerce, Technology Administration, National Institute of Standards and Technology, 2001.

[22] M. E. Vance, T. Kuiken, E. P. Vejerano, S. P. McGinnis, M. F. Hochella, D. Rejeski e M. S. Hull, «Nanotechnology in the real world: Redeveloping the nanomaterial consumer products inventory,» *Beilstein Journal of Nanotechnology,* vol. 6, pp. 1769-1780, 2015.

[23] Y. Li, K. Xiao, J. Luo, J. Lee, S. Pan e K. S. Lam, «A novel size-tunable nanocarrier system for targeted anticancer drug delivery,» *Journal of Controlled Release,* vol. 144, n. 3, pp. 314-323, 2010.

[24] B. Fahmy e S. A. Cormier, «Copper oxide nanoparticles induce oxidative stress and cytotoxicity in airway epithelial cells,» *Toxicology in Vitro,* vol. 23, n. 7, pp. 1365-1371, 2009.

[25] A. Balasubramanyam, N. Sailaja, M. Mahboob, M. F. Rahman, S. M. Hussain e P. Grover, «In vitro mutagenicity assessment of aluminium oxide nanomaterials using the Salmonella/microsome assay,» *Toxicology in Vitro,* vol. 24, n. 6, pp. 1871-1876, 2010.

[26] L. Sárközi, E. Horváth, Z. Kónya, I. Kiricsi, B. Szalay, T. Vezér and A. Papp, "Subacute intratracheal exposure of rats to manganese nanoparticles: Behavioral, electrophysiological, and general toxicological effects," *Inhalation Toxicology,* vol. 21, no. sup1, pp. 83-91, 2009.

[27] G. Oszlánczi, T. Vezér, L. Sárközi, E. Horváth, Z. Kónya e A. Papp, «Functional neurotoxicity of Mn-containing nanoparticles in rats,» *Ecotoxicology and Environmental Safety,* vol. 73, n. 8, pp. 2001-2009, 2010.

[28] M. Singh, H. M. Haverinen, P. Dhagat e G. E. Jabbour, «Inkjet Printing-Process and Its Applications,» *Advanced Materials,* vol. 22, n. 6, pp. 673-685, 2010.

[29] K. M. Tyner, S. R. Schiffman e E. P. Giannelis, «Nanobiohybrids as delivery vehicles for camptothecin,» *Journal of Controlled Release,* vol. 95, n. 3, pp. 501-514, 2004.

[30] E. Horváth, G. Oszlánczi, Z. Máté, A. Szabó, G. Kozma, A. Sápi, Z. Kónya, E. Paulik, L. Nagymajtényi e A. Papp, «Nervous system effects of dissolved and nanoparticulate cadmium in rats in subacute exposure,» *Journal of Applied Toxicology,* vol. 31, n. 5, pp. 471-476, 2011.

[31] H. L. Karlsson, P. Cronholm, J. Gustafsson e L. Möller, «Copper Oxide Nanoparticles Are Highly Toxic: A Comparison between Metal Oxide Nanoparticles and Carbon Nanotubes,» *Chemical Research in Toxicology,* vol. 21, n. 9, pp. 1726-1732, 2008.

[32] M.-T. Zhu, W.-Y. Feng, B. Wang, T.-C. Wang, Y.-Q. Gu, M. Wang, Y. Wang, H. Ouyang, Y.-L. Zhao e Z.-F. Chai, «Comparative study of pulmonary responses to nano- and submicron-sized ferric oxide in rats,» *Toxicology,* vol. 247, n. 2-3, pp. 102-111, 2008.

[33] L. K. Limbach, P. Wick, P. Manser, R. N. Grass, A. Bruinink e W. J. Stark, «Exposure of Engineered Nanoparticles to Human Lung Epithelial Cells: Influence of Chemical Composition and Catalytic Activity on Oxidative Stress,» *Environmental Science & Technology,* vol. 41, n. 11, pp. 4158-4163, 2007.

[34] S. Gunalan, R. Sivaraj e R. Venckatesh, «Aloe barbadensis Miller mediated green synthesis of mono-disperse copper oxide nanoparticles: Optical properties,» *Spectrochimica Acta Part A: Molecular and Biomolecular Spectroscopy,* vol. 97, pp. 1140-1144, 2012.

[35] I. Perelshtein, G. Applerot, N. Perkas, E. Wehrschuetz-Sigl, A. Hasmann, G. Guebitz e A. Gedanken, «CuO–cotton nanocomposite: Formation, morphology, and antibacterial activity,» *Surface and Coatings Technology,* vol. 204, n. 1-2, pp. 54-57, 2009.

[36] F. Perreault, A. Oukarroum, S. P. Melegari, W. G. Matias e R. Popovic, «Polymer coating of copper oxide nanoparticles increases nanoparticles uptake and toxicity in the green alga Chlamydomonas reinhardtii,» *Chemosphere,* vol. 87, n. 11, pp. 1388-1394, 2012.

[37] Z.-s. Hong, Y. Cao e J.-f. Deng, «A convenient alcohothermal approach for low temperature synthesis of CuO nanoparticles,» *Materials Letters,* vol. 52, n. 1-2, pp. 34-38, 2002.

[38] A. S. Lanje, S. J. Sharma, R. B. Pode e R. S. Ningthoujam, «Synthesis and optical characterization of copper oxide nanoparticles,» *Adv Appl Sci Res,* vol. 1, n. 2, pp. 36-40, 2010.

[39] V. R. Kumar, Y. Diamant e A. Gedanken, «Sonochemical Synthesis and Characterization of Nanometer-Size Transition Metal Oxides from Metal Acetates,» *Chemistry of Materials,* vol. 12, n. 8, pp. 2301-2305, 2000.

[40] A. A. Eliseev, A. V. Lukashin, A. A. Vertegel, L. I. Heifets, A. I. Zhirov e Y. D. Tretyakov, «Complexes of Cu(II) with polyvinyl alcohol as precursors for the preparation of CuO/SiO2 nanocomposites,» *Material Research Innovations,* vol. 3, n. 5, pp. 308-312, 2000.

[41] D. Jia, J. Yu e X. Xia, «Synthesis of CuO nanometer powder by one step solid state reaction at room temperature,» *Chinese Science Bulletin,* vol. 43, n. 7, pp. 571-573, 1998.

[42] K. Borgohain, J. B. Singh, M. V. Rama Rao, T. Shripathi e S. Mahamuni, «Quantum size effects in CuO nanoparticles,» *Physical Review B,* vol. 61, n. 16, pp. 11093-11096, 2000.

[43] C. Xu, Y. Liu, G. Xu e G. Wang, «Preparation and characterization of CuO nanorods by thermal decomposition of CuC2O4 precursor,» *Materials Research Bulletin,* vol. 37, n. 14, pp. 2365-2372, 2002.

[44] M. Salavati-Niasari e F. Davar, «Synthesis of copper and copper(I) oxide nanoparticles by thermal decomposition of a new precursor,» *Materials Letters,* vol. 63, n. 3-4, pp. 441-443, 2009.

[45] M. Ikeyama, S. Nakao e H. Masuda, «Formation of fine particles in solid by ion implantation technology,» *Nagoya Kogyo Gijutsu Kenkyusho Hokoku,* vol. 49, n. 2, pp. 151-167, 2000.

[46] S. Honary, H. Barabadi, E. G. Fathabad e F. Naghibi, «Green synthesis of copper oxide nanoparticles using penicillium aurantiogriseum, penicillium citrinum and penicillium wakasmanii,» *Digest J Nanomater Biostruct,* vol. 7, pp. 999-1005, 2012.

[47] G. Ren, D. Hu, E. W. Cheng, M. A. Vargas-Reus, P. Reip e R. P. Allaker, «Characterisation of copper oxide nanoparticles for antimicrobial applications,» *International Journal of Antimicrobial Agents,* vol. 33, n. 6, pp. 587-590, 2009.

[48] N. Strambeanu, L. Demetrovici e D. Dragos, «Natural Sources of Nanoparticles,» in *Nanoparticles' Promises and Risks*, Springer International Publishing, 2015, pp. 9-19.

[49] N. Strambeanu, L. Demetrovici e D. Dragos, «Anthropogenic Sources of Nanoparticles.,» in *Nanoparticles' Promises and Risks*, Springer International Publishing, 2015, pp. 21-54.

[50] The European Communities, «Sustainable Nanotechnologies Project,» 2016. [Online]. Available: http://www.sun-fp7.eu/. [Consultato il giorno 2016 12 20].

[51] R. Korman, «Wanted: new ideas. Panel ponders ways to end accidents and health hazards,» *Engineering News-Record,* vol. 247, n. 27, pp. 26-29, 2001.

[52] M. Behm, «Linking construction fatalities to the design for construction safety concept,» *Safety Science,* vol. 8, n. 589-611, p. 43, 2005.

[53] A. L. Costa, «Rational Approach for the Safe Design of Nanomaterials,» in *Nanotoxicology: Progress toward Nanomedicine, Second Edition*, CRC press, 2014, pp. 37-43.

[54] K. Savolainen, U. Backman, D. Brouwer, B. Fadeel, T. Fernandes, T. Kuhlbusch, R. Landsiedel, I. Lynch e L. Pylkkänen, «Nanosafety in Europe 2015–2025: towards safe and sustainable nanomaterials and nanotechnology innovations,» *Finnish Institute of Occupational Health,* 2013.

[55] M. Zhu, G. Nie, H. Meng, T. Xia, A. Nel e Y. Zhao, «Physicochemical Properties Determine Nanomaterial Cellular Uptake, Transport, and Fate,» *Accounts of Chemical Research,* vol. 46, n. 3, pp. 622-631, 2013.

2 DEVELOPMENT OF SbyD STRATEGIES CANDIDATES

My design strategy was applied to commercial pristine CuO NPs that were modified with the addition of different coating agents, adsorbed by self-assembling. In this CHAPTER 2 are described materials and methods used for obtaining modified samples and allowing a comparison with pristine ones through characterisation at dry state (CHAPTER 3), at wet state (CHAPTER 4), characterisation of HAZARD related properties (CHAPTER 5) and of performances (CHAPTER 6).

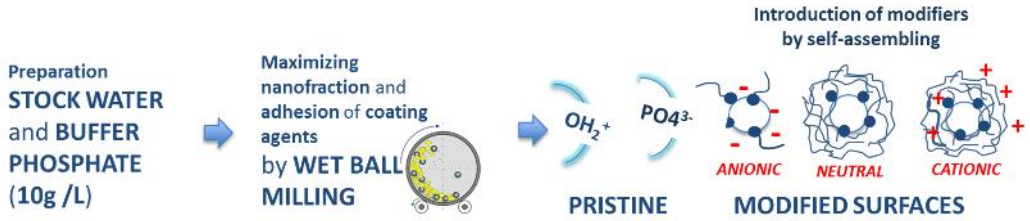

Figure 2.1_ Overall view of Design Strategy

In figure 2.1 is summarized the proposed common process between each strategy:

1. The material is firstly dispersed in convenient media.
2. The nanofraction is freed in the presence of the coating agent to promote the saturation of the material surface.
3. The obtained material is tested and compared with the others and with the pristine.

2.1 Selection of CuO NPs as case study

Copper-based formulations have been widely used for several years particularly in ground contact applications to treat timber due to their effectiveness as a biocide and low mammalian toxicity [1], [2]. The biocidal mechanism of copper-based formulations is based upon the cupric ion's interference with homeostatic processes and cell membrane functions, protein and enzyme damage and precipitation, production of reactive oxygen species and DNA disruption. Copper is the only biocide that successfully inhibits wood decomposition by soft rot fungi [3]. Key limitations of copper based wood preservation formulations include lack of efficacy to treat some

copper tolerant wood destroying fungi (Basidomycetes, fungi included in genera Serpula and some fungi species once included within the genus Poria), refractory wood species (e.g. several species of fir) [4], [2] and aquatic toxicity [2].
Wood preservation treatment is indispensable to increase the service life of timber through bactericidal, fungicidal and insecticidal agents [2], [1]. Improving the efficacy of wood preservation treatments and ability to use a variety of timber species can limit deforestation and save human labour to build essential infrastructure [5]. While impregnation of wood with chemical preservatives using pressure treatment is the most effective way to achieve good penetration and retention, surface treatments may also be used when lesser protection is required, if pressure treatment is not practicable for any reason or for consumer based applications. Non-pressure treatments include non-pressure impregnation (e.g. brief dipping, cold soaking and steeping, diffusion processes, vacuum processes) and in situ treatments (e.g. surface treatments using spraying, brush and paste application, installation of internal diffusible chemicals, internal fumigant treatments) [1].

This case study examines a hypothetical nano-enabled biocidal white paint, manufactured in Germany by BASF, for consumer based application: coating of a wooden garden fence. The function of this coating is to protect a wooden fence consisting of poles and boards in contact with ground and fully exposed to the weathering. In addition to weathering protection provided by the acrylic paint, the paint containing CuO NPs also provides a biocidal functionality (decay by microorganisms especially soft rot fungi) to the softwood cladding.

2.2 Preliminary dataset collection on target material

The copper oxide nanoparticles were produced by PlasmaChem GmbH (Berlin, Germany) with the following method: The copper inorganic precursor (copper hydroxycarbonate, $Cu_2(OH)_2CO_3$) is freshly synthesized from 1M copper nitrate solution and sodium carbonate and then dried at 100°C. The dried milled precursor

is then decomposed in air at ca. 350°C according to the manufacturer reserved protocol: several hours with periodical slight mixing during the decomposition. Cooling to mild temperatures (100-150°C) is performed in an oven; afterwards the material is cooled down to room temperature.

Chemical yield of process is close to 100% and energy consumption for the manufacture was 13.8 kWh per material kilogram.

The characteristics of CuO NPs (Figure 2.2) as reported by the manufacturer are:

- Cu (II) oxide nanopowder (CuO),
- Spherical,
- Average primary particle size: 15nm (XRD crystallite size)
- BET (Brunauer, Emmett and Teller) surface area 45±5 m^2/g
- 99.9% (No organic stabilizers added)
- Monoclinic crystal system (Tenorite)
- Density: 6.3 g/cm^3 (Bulk material: 6.5 g/cm^3)
- Shipped as dry powder

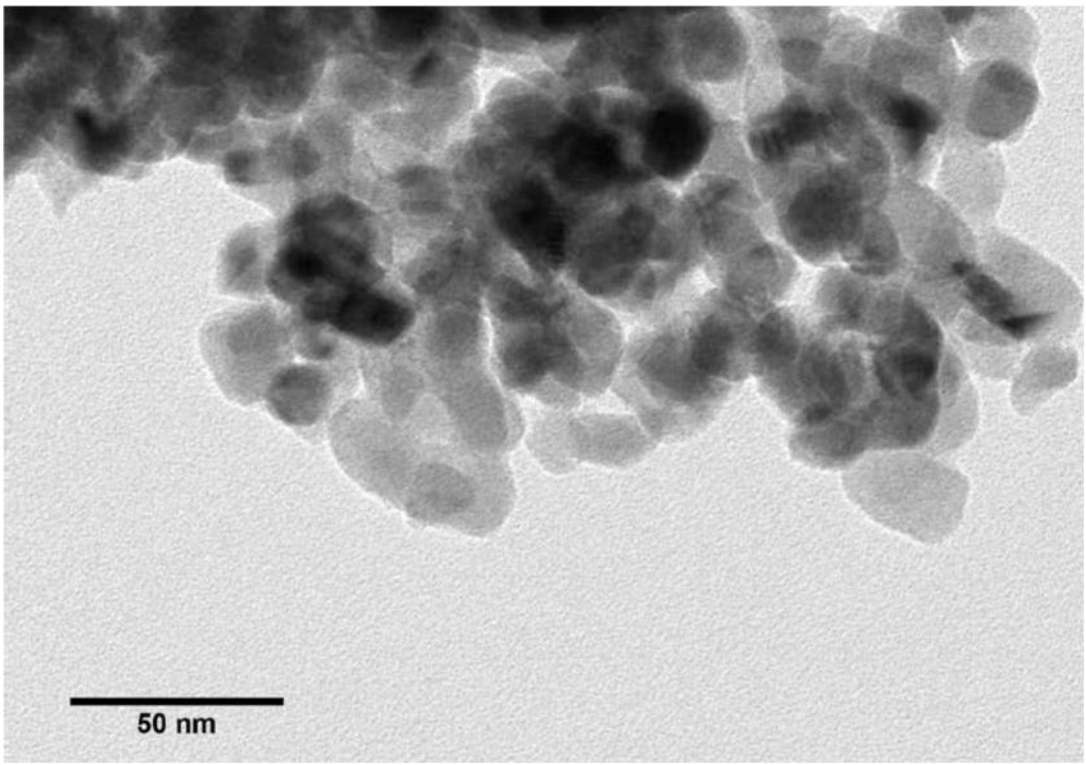

Figure 2.2 TEM microscopy of the CuO NPs as provided

2.3 Selection of surface modifiers

Different coating agents are currently employed for the functionalization of metals and metal oxide NPs surfaces. Coating the particles by self-assembling techniques, taking advantage of weak acid-base or hydrogen bonding interactions [6], [7] between the selected agents and the reactive species on the particle surface, allows to rapidly achieve the saturation of the active spots in a single-step reaction. The surface modification is expected to provide two main effects:

1. Colloidal stabilization, because of the modified particle-particle interaction at the surface there will be stronger repulsion that reduces the overall aggregation and promotes particle dispersibility
2. Cations leaching control, the local dissolution phenomenon (leaching) due to the interaction between active surfaces and dispersion media, that is considered the principal route to toxicity [8], will be shielded by the presence of a third agents in the interface.

For the present investigation, I selected four coating agents (figure 2.3) able to bind themselves with CuO NPs surface and bringing different modifications to the surface chemical identity: positively charged (branched polyethyleneimine, B-PEI); neutral (polyvinylpyrrolidone, PVP); negatively charged (sodium citrate); negatively charged with strong reductive capacity (sodium ascorbate). In this way, I could observe different effects arising from the induced different surface chemistry and inspect if any of these alterations is capable to mitigate the material risks.

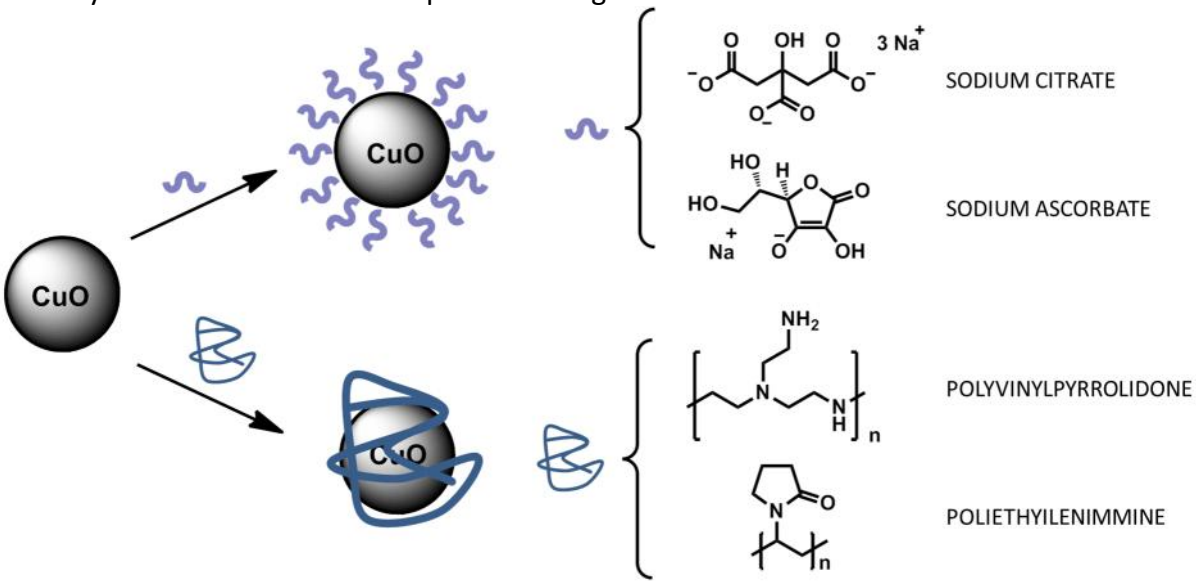

Figure 2.3_Schematic representation of SbyD strategy applied: introduction of modifying agents (i.e. CIT, ASC, PEI and PVP) by self-assembling.

2.4 Identification of the best amount of modifier through Zeta potential titration

Exploiting the coating agents' ability to change surface electrical properties, I performed Zeta potential titrations of CuO NPs suspensions adding each modifying agent individually. Since the modifiers will preferably bind to free surface areas, gradually changing the particle properties, in this titration will be shown a plateau value on the Zeta potential curves that corresponds to the particle charge after surface saturation. The modifier concentration where the plateau starts is the minimum amount necessary to saturate the surface (best amount, figure 2.4) [9].

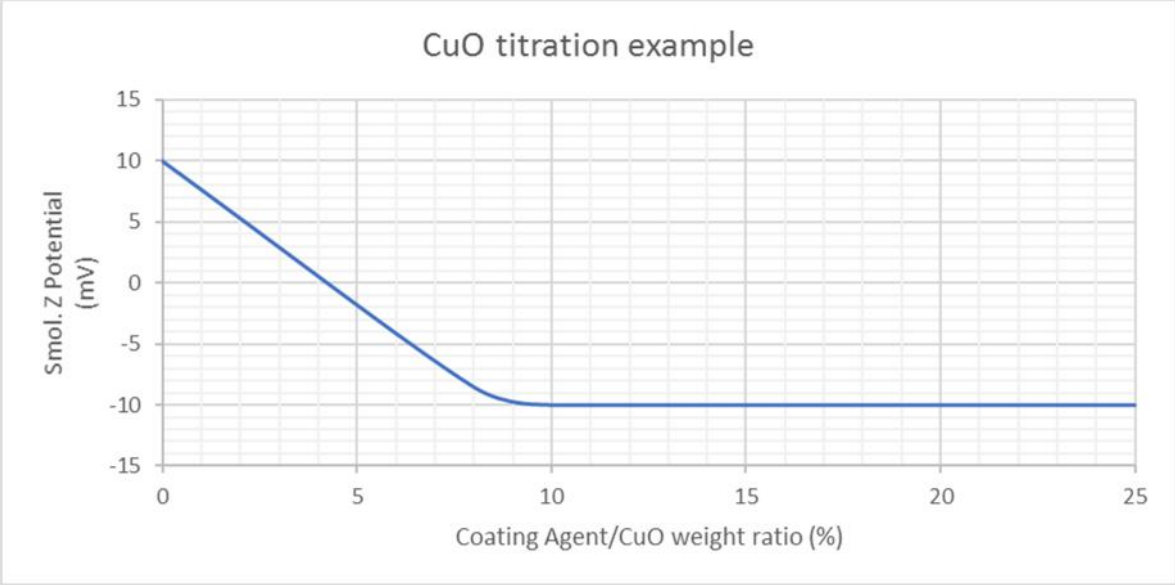

Figure 2.4_Titration example with a hypothetical negative coating agent. The Best amount is identified at 10% weight ratio.

Method: The titration was performed for each coating agent separately, with an electroacoustic technique (Acoustosizer, Colloidal Dynamics) on 100ml of NPs in water suspension prepared at 10 wt. % in CuO powder. The modifier solution is prepared at 0.175g/l and is slowly added to the solution, with increments of 0,2 ml up to 10 ml. During the titration both Z-potential and particle size distribution are recorded.

2.5 Selection of the Buffer systems

According to Cho [10], CuO NPs are rapidly and completely dissolved at pH of 5.5 and the CuO NPs suspension in water (without additives) exhibited values only slightly less acidic: 6.4. Solubility experiments were conducted by producing suspensions at different pH values with HCl and NaOH, the determination of dissolved copper was carried out after magnetic stirring for 24h after the pH alteration. The results confirmed the tendency of copper oxide NPs to dissolve in acid environment, as shown in the following chart (Figure 2.5).

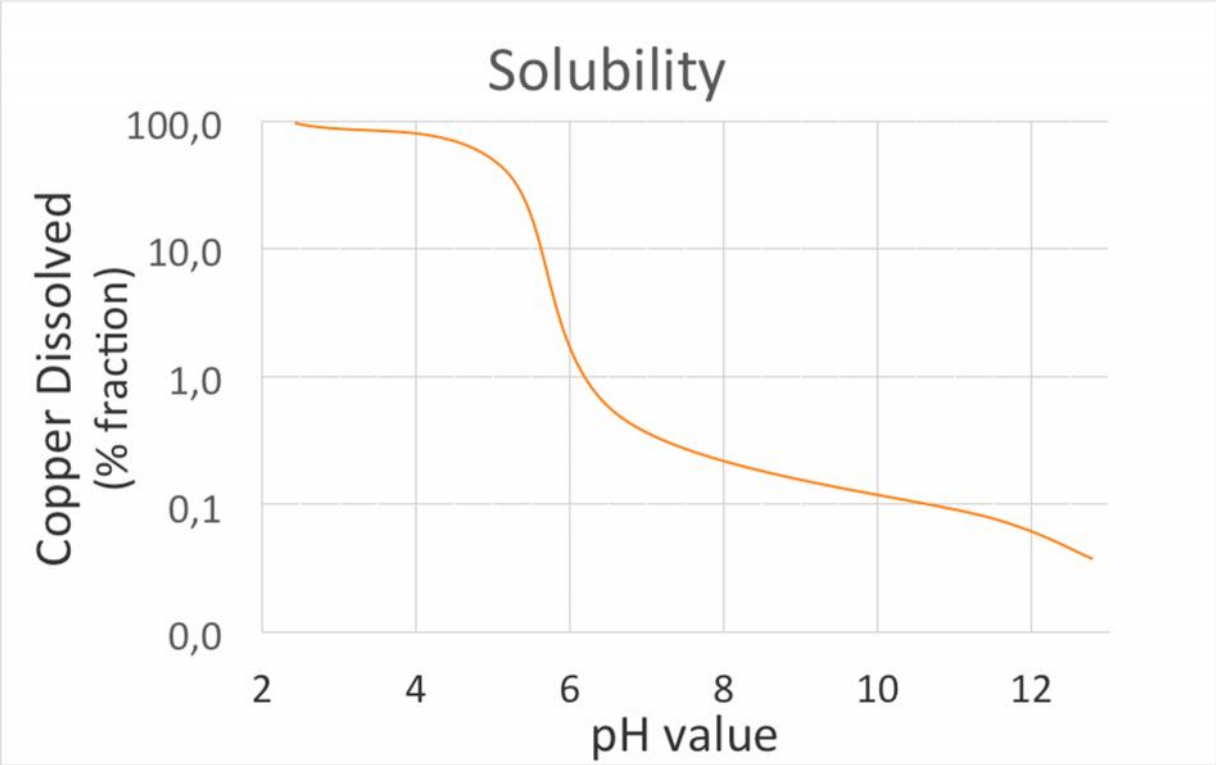

Figure 2.5_pH effect on solubility for CuO NPs

The testing suspension were therefore reformulated with the addition of Boric acid/sodium borate buffer, getting the *buffer(borate) suspension* with pH buffered at 9.14. This buffer has been chosen because capable of maintaining the solution alkaline and avoiding coper dissolution without reacting with copper oxide. Later the *buffer(phosphate)* solutions were also produced because borate natural antibacterial quality was interfering with toxicological assays.

2.6 Handling protocols

2.6.1 Colloidal dispersions

Dispersion protocol is a critical part of design and testing strategies and is necessary to compare dry pristine powder with wet modified samples.

A summary of the produced samples useful for the evaluation of safer by molecular design strategies is reported in Table 2.1. Steps made to collect and modify samples are schematically reported in Figures 2.6-2.8.

Table 2.1_Pristine and modified samples

Type	Code	Phys. State	MEDIUM
PRISTINE SAMPLES			
PR	CuO_1	Powder	
	CuO_24	Sol	Ultrapure H_2O
	CuO_92	Sol	Na Borate buffer
	CuO_106	Sol	Na Phosphate buffer
MODIFIED SAMPLES: BALL MILLING			
BM	CuO_91	Sol	Ultrapure H_2O
	CuO_94	Sol	Na Borate buffer
	CuO_101	Sol	Na Phosphate buffer
	CuO_107	Freeze dried Powder	Na Phosphate buffer
MODIFIED SAMPLES: ORGANIC COATING			
CIT	CuO_33	Sol	Na Borate buffer
PVP	CuO_38	Sol	Na Borate buffer
PEI	CuO_43	Sol	Na Borate buffer
ASC	CuO_78	Sol	Na Borate buffer
MODIFIED SAMPLES COATING + BALL MILLING			
CIT-BM	CuO_110	Sol	Ultrapure H_2O
PVP-BM	CuO_111	Sol	Ultrapure H_2O

PEI-BM	CuO_112	Sol	Ultrapure H_2O
ASC-BM	CuO_113	Sol	Ultrapure H_2O
CIT-BM	CuO_53	Sol	Na Borate buffer
PVP-BM	CuO_63	Sol	Na Borate buffer
PEI-BM	CuO_73	Sol	Na Borate buffer
ASC-BM	CuO_88	Sol	Na Borate buffer
CIT-BM	CuO_102	Sol	Na Phosphate buffer
PVP-BM	CuO_103	Sol	Na Phosphate buffer
PEI-BM	CuO_104	Sol	Na Phosphate buffer
ASC-BM	CuO_105	Sol	Na Phosphate buffer
PEI-BM	CuO_108	Freeze-dried Powder	Na Phosphate buffer
ASC-BM	CuO_109	Freeze-dried Powder	Na Phosphate buffer
MODIFIED SAMPLES GRANULATION			
SD	CuO_95	Powder	
	CuO_98	SD powder re-dispersed	Ultrapure H_2O
MODIFIED SAMPLES BALL MILLING + GRANULATION			
BM-SD	CuO_96	Powder	
	CuO_99	SD powder re-dispersed	Ultrapure H_2O
MODIFIED SAMPLES COATING + BALL MILLING + GRANULATION			
ASC-BM-SD	CuO_97	Powder	
	CuO_100	SD powder re-dispersed	Ultrapure H_2O

Samples category:
Pristine: **PR** (as received powder, or dispersed by US)
Coated: **CIT** (Citrate); **PVP** (Polyvinylpyrrolidone); **PEI** (Polyethylenimine); **ASC** (Ascorbate)
Ball milled: **BM** (ball milling treatment 95h)
Spray-dried: **SD** (granulation via spray drying treatment)

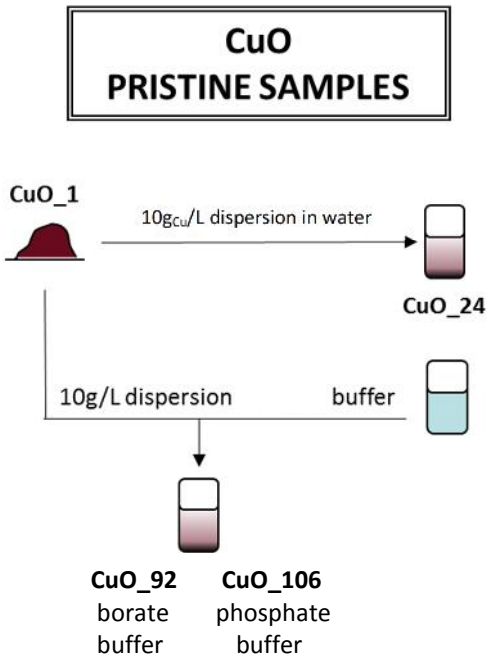

Figure 2.6_Pristine samples preparation scheme

For every experiment, when a buffered solution is used, it has been prepared at 50mM strength either with the boric acid/sodium borate couple (pH 9.14) or with the Na_2HPO_4/Na_3PO_4 (pH 7.4).

The pristine samples were prepared at 10g/L of elemental copper, by weighting 1252 mg of provided CuO powder into a 100 ml volumetric flask, therefore 12.5 g/L in CuO. The flask is then filled with water or one of the two buffer solutions.

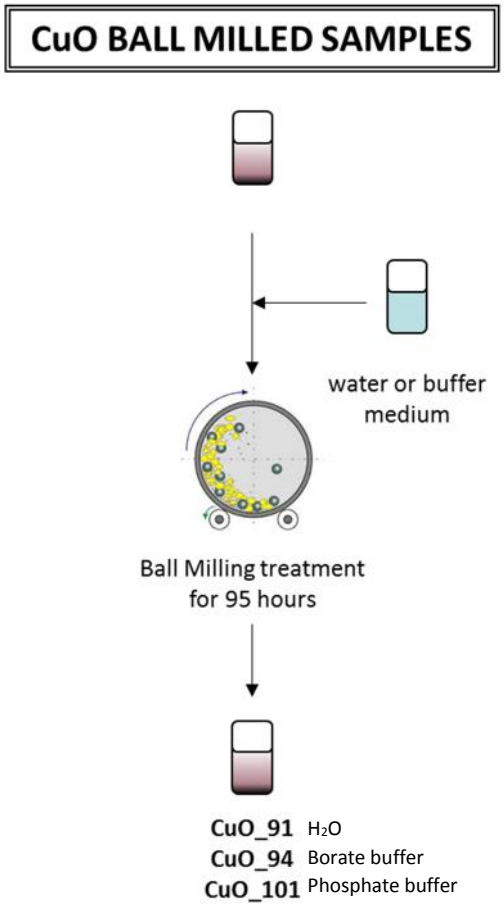

Figure 2.7_Ball milled samples preparation scheme

Each sample treated with low energy grinding (wet ball milling) was obtained by adding to 100ml of the suspensions obtained as described in the previous step (figure 2.4), 50ml of 2mm YTZ grinding media (yttrium stabilized with zirconium spheres). The best fragmentation was obtained after 95 hours of treatment.

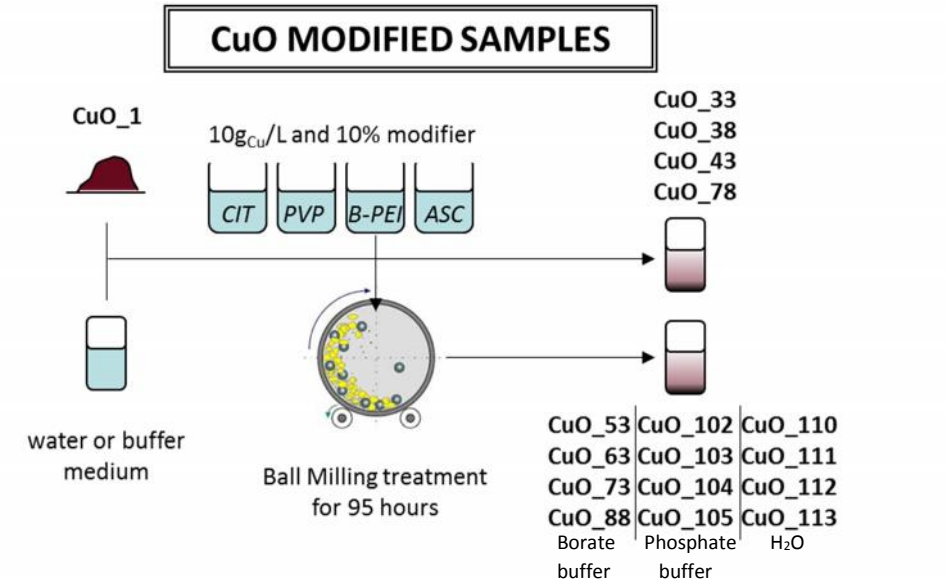

Figure 2.8_Modified samples preparation scheme

Modified samples were obtained by extending the already exposed dispersion and, if required, grinding process to comprehend the addition of the correct amount of selected modifiers.

2.6.2 Solid powders recovery

Spray drying and freeze drying are typical powder treatments of the ceramic process usually performed in order to control water removal by improving particle homogeneity. These procedures are required to merge the modified product back into the industrial processes because the CuO NPs are stocked, shipped and employed as solid powders. Freeze-drying works by freezing the material and then reducing the surrounding pressure to allow the frozen water in the material to sublimate directly from the solid phase to the gas phase. During spray drying the suspension is sprayed by a nozzle into a hot air current, in this way the drops are instantaneously dried and granulated. The application of such spray-granulation techniques to ceramic nanosols is a new and powerful technology to obtain the following structures:

- Micron-submicronic spherical agglomerates/aggregates of powders that preserve their primary nanostructure even though resulting in being easier to handle and less dusty;
- Templant or encapsulating micro/sub micrometric structures for organic (drugs, additives) or inorganic (nanoparticles) moieties nanostructure;

Spray granulation techniques have been successfully applied in the Sanowork project to agglomerate/aggregate powders and control their aerosolizing during manufacturing steps such as powder recovery, handling, weighing, stocking or drying. They have been proposed as “nano in micro” design options and evaluated in terms of reduced dustiness and preserved or improved properties [11]. The same approaches have been re-proposed in the SUN project and I have followed the preparation of the sample powders.

Powders, once spray-dried, were re-dispersed in order to check if the nano-fraction that was made available after ball milling could be released after spray-drying. The knowledge of dispersibility after spray-granulation is very important in order to evaluate performance and biological identity of samples introduced again in a wet medium.

Method:

Freeze-drying: This process was done by collecting 250ml of the selected 10g/L CuO NPs suspension into a steel container (diameter 25 cm, height 9 cm). The container is then immersed for half of its height in liquid nitrogen until completely frozen. The container is then inserted in a freeze drier with controlled temperature and pression, these parameters and the dwell time were adjusted for each sample.

Spray-drying: granulation was performed by using bench-top spray-drier equipment (Spray-dryer SD-05, Lab-Plant Ltd., Huddersfield, England). The selected stock solution was fed at 480 ml/h from a mechanical stirred becher and nebulized through a 500 µm nozzle with pressurized air at 1.8 bar in a counter current system with hot air at a temperature of 250°C.

2.7 STRUCTURAL AND SURFACE PROPERTIES ANALYSIS (SYNTHETIC IDENTITY DEFINITION)

The first tool required to understand nanoparticles behaviour is an image of the material, this gives the first hints about the particle morphological properties, aggregation state, size and size distribution. These images were collected by electronic microscopy.

After the particle suspension has been produced and the surface modification has been applied it is necessary to ensure that the coating agents is bound to the particle surface, through thermogravimetric analysis, and that it has changed only the surface without further reaction with the particle, through XRD analysis.

2.7.1 Electronic microscopy analysis

Method:

FE-SEM analysis: Suspensions for FE-SEM microscopy (Sigma-Zeiss) were prepared by properly diluting the stock solutions in the final media, in order to reach a final concentration in the range 50-100 ppm, and drying a small amount of suspension on a steel stub with silicon chip, by IR light exposure for 30 minutes. The type of detector and level of magnification was explored for each sample in order to collect better images at different magnification.

STEM analysis: Transmission electron detector unit (STEM) images were collected with the same FE-SEM instrument described above. The samples were observed in the transmission mode at 30 kV. Specimens of CuO for STEM investigations were prepared by diluting the nanosuspension with water (1:100) and depositing a drop on a metallic grid, then evaporating it in air at room temperature.

2.7.2 Thermogravimetric analysis

Method: The evaluation of the coating agent amount adsorbed on CuO NPs surface was performed by thermal analysis on the dried CuO modified samples. In order to distinguish the adsorbed coating agent from the free one, the free modifier was eliminated by ultrafiltration of the stock suspensions (10 g_{Cu}/L) and the adsorbed agent quantified by thermogravimetric analysis on the dried CuO powders. The weight loss percentage of the ultrafiltered (UF) and not ultrafiltered (NO UF) modified samples were compared and normalized with respect to the pristine sample loss and to the phosphate coated sample loss in order to evaluate the amount of the coating inclusive of phosphate or not. The free modifiers can be estimated as the difference between the total modifier amount detected on the not filtered samples and the adsorbed coating agent amount detected on the ultrafiltered ones.

2.7.3 XRD characterization of pristine and modified samples

Methods:

The phase composition of the CuO nanopowders was determined by X-ray diffraction (XRD) collecting patterns of dried powders of the samples pristine and modified with ionic agents (CIT, ASC and B-PEI). Each suspension was dried for 24 h at room temperature in air, washed several times with absolute ethanol and dried in oven at 130◦C for 10 min. Analyses were performed by a diffractometer Bruker D8 Advance (Germany) operating in θ/2θ configuration, with a LinxEye detector (10–60°2θ range, 0.02 step size, 8 s equivalent time-per-step).

2.8 COLLOIDAL PROPERTIES ANALYSIS (EXPOSURE IDENTITY DEFINITION)

The colloidal characterization of nanopowders is essential to provide a biological identity for samples tested in (eco) toxicological assays and support the development of surface engineering practices since those are built on colloidal self-assembling techniques.

When considering the life-cycle of the system during sampling and testing procedures it must be noted that the produced engineered nanoparticles will cross many different media experiencing physicochemical evolution, the change of colloidal properties is outlined in Figure 2.9.

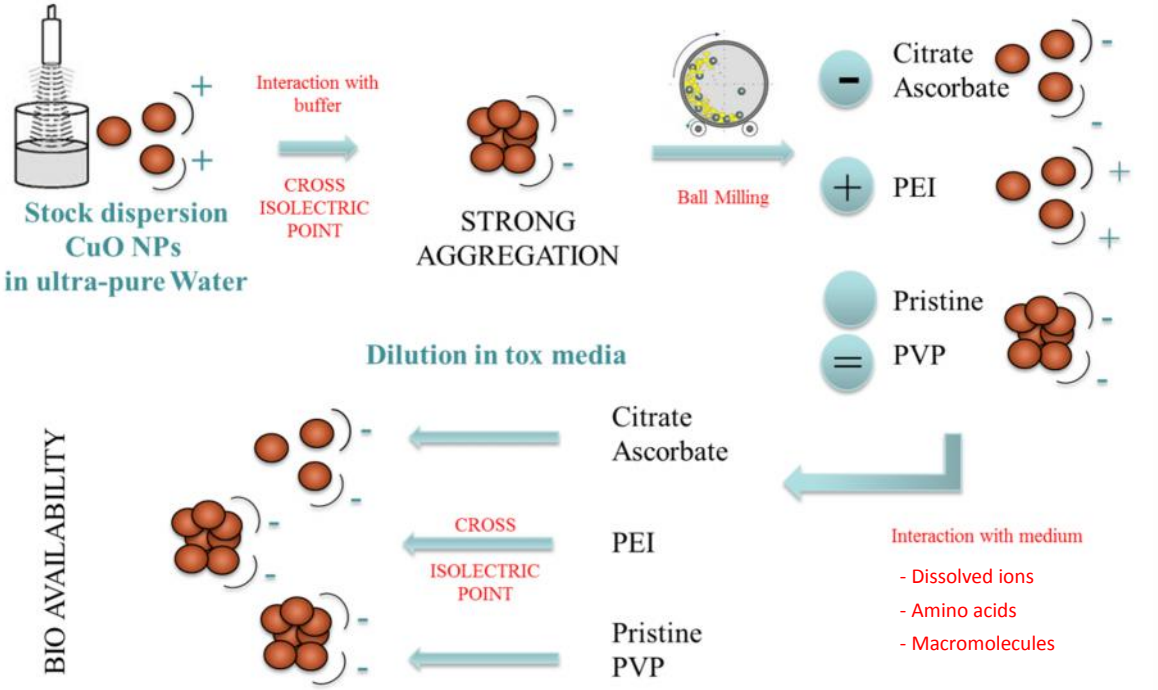

Figure 2.9_CuO NPs life-cycle evolution in sampling and testing media (destabilisation justified by i.e.p. crossings)

The crossing of i.e.p. always induces a strong aggregation that requires mechanical grinding to be reversed, this phenomenon may be usefully exploited also in terms of safety by design strategy because can limit potential NPs risk: aggregated cluster in fact have reduced mobility, with immediate reduction of exposure, and loose also the ability to cross cellular membranes, limitation that can hinder the nano-related toxicity pathways.

2.8.1 Testing media

Suspensions for wet state characterization were prepared by properly diluting the stock suspensions in the final media, in order to yield a final concentration in the range 50-100 ppm.

Experimental media were ultrapure water, as a reference media, and other solutions, reported in tables 2.2 and 2.3, as medium for biological or environmental exposure simulation.

Table 2.2_Concentration of inorganic salts (g/L) in Dulbecco's Phosphate Buffered Saline (PBS), biological (MEM and DMEM) and environmental (AFW and AMW) media.

	PBS	**MEM**	**DMEM**	**AFW**	**AMW**
Inorganic salts	(g/L)	(g/L)	(g/L)	(g/L)	(g/L)
$CaCl_2 \cdot 2H_2O$	0.133	0.265	0.264	0.294	1.47
$Fe(NO_3)_3 \cdot 9H_2O$	-	-	0.0001	-	-
$MgSO_4$ (anhydrous)	-	0.098	-	-	-
$MgSO_4$ $7H_2O$	-	-	0.2	0.123	-
$MgCl_2 \cdot 6H_2O$	0.1	-	-	-	10.8
KCl	0.2	0.4	0.4	0.006	0.7
KH_2PO_4	0.2	-	-	-	-
$NaHCO_3$	-	2.2	3.7	0.064	0.2
NaCl	8	6.8	6.4	-	23.5
Na_2HPO_4 (anhydrous)	1.15	-	-	-	-
NaH_2PO_4 (anhydrous)	-	0.122	-	-	-
$NaH_2PO_4 \cdot 2H_2O$	-	-	0.141	-	-
Na_2SO_4	-	-	-	-	4.0
$SrCl_2$ 6H2O	-	-	-	-	0.02
H_3BO_3	-	-	-	-	0.03
KBr	-	-	-	-	0.10
Na_2O_3Si $9H_2O$	-	-	-	-	0.02

Table 2.3_Concentration (g/L) of amino acids in biological media: MEM and DMEM.

	MEM	**DMEM**
Amino acids	(g/L)	(g/L)
Glycine	-	0.03
L-Arginine · HCl	0.126	0.084
L-Cystine · 2HCl	0.0313	0.063
L-Glutamine	0.292	0.58
L-Histidine · HCl · H_2O	0.042	0.042
L-Isoleucine	0.052	0.105
L-Leucine	0.052	0.105
L-Lysine · HCl	0.0725	0.146
L-Methionine	0.015	0.03
L-Phenylalanine	0.032	0.066
L-Serine	-	0.042
L-Threonine	0.048	0.095
L-Tryptophan	0.01	0.016
L-Tyrosine · 2Na · $2H_2O$	0.0519	0.072
L-Valine	0.046	0.094
	(g/L)	(g/L)
Glucose	1	4.5
Phenol red ·Na	0.011	0.015
Sodium Pyruvate	-	0.11

2.8.2 Isoelectric point

The identification of the pH value where Zeta potential reaches neutrality (isoelectric point, i.e.p.) allows the formulation of a hypothesis on the type of charged molecules specifically adsorbed on the surface and as well on the type of agglomeration.

Zeta Potential values of metal oxide nanoparticles depends on their surface acid or base properties, modified by the presence of specifically adsorbed coating agent or by their state of agglomeration. As already reported, the degree of agglomeration is associated to a different capability of stabilizing conjugated acid or base substances, causing a shift of isoelectric point towards the acidic or basic region. This means that the same compound at the same pH can express lower or higher values of Zeta potential or can reverse sign if the pH observed stays centred between two different isoelectric points. A schematic representation of this situation is represented in Figure 2.10.

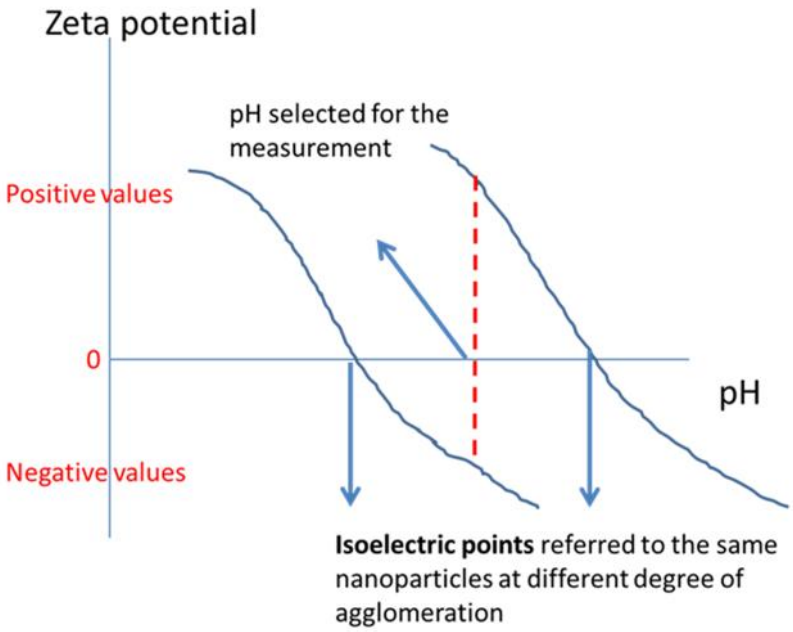

Figure 2.10_Representation of isoelectric point shift for the same NPs due to agglomeration degree changes.

It can be observed from the theoretical example reported in this chart how the shift of isoelectric point towards the acidic region corresponds to Zeta potential reversing sign from positive to negative. In general, more aggregated powders show a lower value of Zeta potential as absolute value, indicating a shift of i.e.p. towards the acidic region for naturally positive Zeta potential and towards the basic region for naturally negative Zeta potential.

Method:

Isoelectric point: Zeta potential vs pH titration was performed by SUN partner UNIVE, in order to identify the isoelectric point. The Zeta potential values were measured using the Nicomp 380 ZLS instrument. Suspensions of CuO NPs were prepared at 500ppm. The pH of each suspension was determined after vortex mixing and adjusted with 0.1 M HCl or NaOH in order to prepare suspensions with different pH values, in the range from 1.5 to 12.5.

2.8.3 Zeta potential

The Zeta potential of nanoparticles suspension is a key descriptor for predictions on surface reactivity and allows correlation between NPs intrinsic properties and their colloidal stability and biological reactivity because controls:

- Electrical stabilization; with increased surface charge comes a stronger colloidal dispersion, this may improve the material handling and performances while it may also amplify the exposure risk, promoting mobility of the particles in the environment.
- Cellular uptake; biological recognition and absorption of NPs through cell membranes is guided by surface potential interactions [12].
- Fate; considering environmental media pH values, it is possible to re-arrange NPs surface in order to cross the isoelectric point and force agglomeration and phase separation of the particles to reduce mobility.

- Wettability; surface charge has been proven to affects both static wettability and wetting kinetics [13] while surfactant adsorption may even lead to hydrophilic particles (such as metal oxide) inversion to hydrophobic [14].

Method:

Single Zeta potential measurement: Electrophoretic light scattering (ELS) spectra were collected on pristine and modified suspension using Malvern Zeta Sizer instrument. Folded cells were rinsed thoroughly with water, followed by ethanol, and water again, each cell was disposed after analysis. 1 ml of the suspension was added in the folded cell for measurement using a micropipette with disposable tip removing any air bubble. The analysis was performed at 25 °C with an equilibrium time of 2 minutes. A minimum of 10 replicates with 3 measurements per replicate was used.

2.8.4 Particle Size Distribution

The particles size is a key descriptor of nanoscale reactivity and for this reason is included in the EC definition of nanomaterial. The identification of nanomaterials requires accurate measurements of size and concentration by number, accounting for agglomerates and aggregates; industrial nano-powders are spread into a large size population, described by the particle size distribution (PSD). This descriptor affects very important industrial and consumer products properties such as, the setting time of cements, the hiding power of pigments, the activity of catalysts, the taste of food, and the sintering shrinkage of metallurgical compositions. The relevance to toxicology is that the colloidal stability and therefore the biological route for the substance uptake (e.g., bioavailability) are strongly affected by the particle size distribution in biological or environmental relevant media [15].

The knowledge of PSD of NPs dispersed in aqueous media should be necessarily coupled with information on primary particles size and degree of agglomeration in order to provide mechanistic justification of nano-scale reactivity:

1. **Primary particles**. isolated particles. Usually not obtained from industrial processes as their formation is favoured in highly diluted synthesis.
2. **Aggregates**. Clusters of primary particles tightly bound together by rigid chemical bonding, the force necessary to break those clusters is considerable. For most of the industrial nanopowders, aggregates are the largest single fraction of the particle size distribution.
3. **Agglomerates**. These clusters are collections of particles or aggregates loosely held together by weak forces. They can readily be broken apart with proper dispersion techniques like ultrasonic mixing.

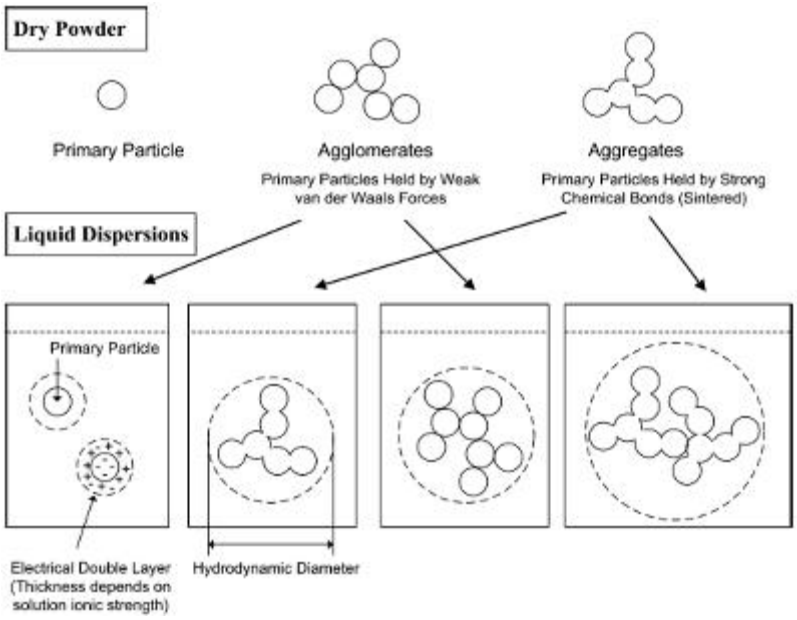

Figure 2.11_Representation of agglomeration, aggregation and EDL effect on the hydrodynamic diameter

Particle size can be described by diameter only for perfect spheres. Real powders often have close to spherical geometry but diameter measures are always to be considered an approximation of the effective condition. One more relevant characteristic of wet state PSD determination is that it gives the average result from a population of particles but is influenced by the dispersing medium: since the

electric double layer at particles' surface forms, around every particle and every cluster there is a region of attracted molecules. Wet-state size determination techniques like dynamic light scattering (DLS), employed in this work, focus on the relationship between PSD and Brownian motions, providing as out-put the hydrodynamic diameter, defined as the diameter of a sphere that has the same diffusion coefficient as the measured one (figure 2.11).

Method:

DLS analysis was performed with Malvern Zeta Sizer instrument. 1.5 ml – 2 ml of the suspension were added in the cuvette for measurement. The analysis was performed at 25 °C with an equilibrium time of 2 minutes. A minimum of 5 replicates with 3 measurements per replicate was used.

Average Agglomeration number (AAN) the AAN was determined according to NIST (see 1.2.4), using D_{50} derived from DLS PSD determination while ρ and SSA are provided by the material manufacturer.

2.8.5 Sedimentation velocity

Method: Colloidal stability was investigated by SUN UNIVE partner with LUMiSizer 651 instrument, calculating the average sedimentation velocity (ASV) of the CuO NPs previously dispersed at 100 mg/L, in order to achieve a good intensity signal, in ultrapure water, PBS, MEM, DMEM, AFW and AMW. AVS is determined at gravity and at 25 °C. For each analysis, the instrument records also PSD (not reported) useful for colloidal stability in AFW interpretation.

2.9 IONS DISSOLUTION/SPECIATION ANALYSIS and TOXICOLOGICAL END-POINTS EVALUATION (HAZARD IDENTITY DEFINITION)

2.9.1 Solubility rate

Method:

ICP analysis: 15 ml of target suspension is centrifugal ultrafiltered (10KDa Millipore filters, 5000RPM, 10 minutes) and supernatant fraction is collected. In order to solubilize the material, every collected sample underwent an acid digestion process. The acid mixture employed (acids of suprapur grade) depends on the material, in some cases different number of samples and different kind of digestion procedures were tested, including microwave assisted digestions.

The obtained solutions are analysed with Agilent Technologies 5100 ICP-OES. Acceptance criterion for the calibration curves was $R^2 \geq 0.995$. The calibration range varied according to the expected concentration of the element in the samples.

Solubility test apparatus: in order to simulate NPs behaviour in relevant media a laboratory incubator capable of maintaining desired temperature for many samples at the same time was set up. The studied samples were obtained by diluting each modified *buffer(phosphate)* suspension into one of the above-mentioned media. The incubation was kept at 20 °C for environmental suspensions and at 37 °C for in vivo and in vitro suspensions, with ultrapure water samples analysed together as reference.

The suspensions were separated by the supernatant after 1h and 24h of incubation, the Cu^{2+}/Cu_{tot} ratio is determined after acid digestion and ICP-OES determination, compared with the total digestion of the generating suspension (figure 2.12).

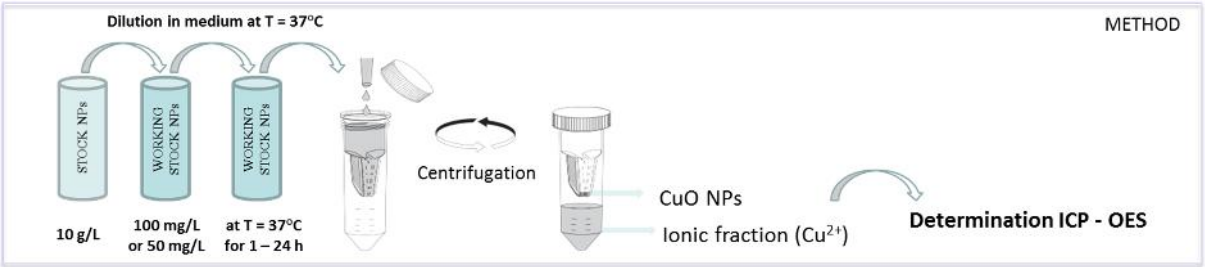

Figure 2.12_Representation of solubility assay preparation method

2.9.2 Electroanalytical methods: a powerful tool towards ion speciation

Although the ICP-OES method is highly reliable, it presents some drawbacks in fact it is disruptive and time consuming. In order to overcome these problems an electroanalytical method, exploiting a three electrode system, has been developed, allowing the detection of Cu^{2+} in CuO aqueous suspensions, this way Cu^{2+} ions can be revealed in situ even in biological media.

Method:

Electroanalysis at the Au electrode has been employed to detect and quantify copper ion leaching in various biological media. Calibration curves of Cu^{2+} in all media were obtained by correlating the known nominal concentration of Cu with the height of anodic peaks appearing during cyclic voltammetry (CV) scans. Cu^{2+} ions were added to the media as copper chloride ($CuCl_2$) solution, up to 200 μmol nominal Cu^{2+} concentrations. Four different toxicological artificial standard media were studied:

- ALDRICH D4031 saline buffer
- ALDRICH D8662 saline buffer
- THERMO FISCHER DMEM high glucose, pyruvate
- Foetal bovine serum-added DMEM (FBS-DMEM)

2.9.3 (Eco) toxicity benchmark

2.9.3.1 In vitro toxicity

Method: The cytotoxic potential of the nanomaterial was investigated by SUN partner Heriot Watt University, using the Alamar Blue cell viability assay. Cells were exposed to increasing concentration of the nanomaterials (from 0 µg/ml to 125 µg/ml) for 24h. The results raw data were used to calculate the benchmark dose 20 (BMD20) and the EC50 for each NM by PROAST 38.9 package software.

2.9.3.2 In vivo eco-toxicity

Method: The common pond snail *L. stagnalis* is a good biomonitor for metal pollution given its capacity to accumulate metals, its suitable size for metal analysis and its wide distribution [16]. These studies have shown that for several metals (Co, Pb, and Ni) *L. stagnalis* is either the most sensitive or second most sensitive invertebrate tested to date [17].

Tests with *L. stagnalis* started with the investigation of the toxicity for the provided material. Acute lethal effects of the different speciation of copper either in the form of aqueous salt $CuSO_4*5H_2O$ (BDH Prolabo®) or CuO NPs (PlasmaChem GmbH) were assessed by SUN partner Heriot Watt University through aqueous exposures by monitoring the mortality in a controlled light (16h day, 8h night) and temperature (20 °C) environment, following the protocol applied by other groups [17]. Briefly, juvenile snails (7-9 day old) were placed in 35ml plastic containers with 30ml of test medium; three replicates of 15 snails were tested for each exposure concentration. Snails were left without food 24h prior the start the experiment. Exposure was performed over 96h, mortality recorded daily and snails were not fed during the experiment.

2.10 References

[1] S. Lebow, «Alternatives to chromated copper arsenate (CCA) for residential construction,» *Madison,* 2004.

[2] M. H. Freeman e C. R. McIntyre, «A comprehensive review of copper-based wood preservatives,» *Forest Products Journal,* vol. 58, n. 11, p. 6, 2008.

[3] C. Civardi, F. W. Schwarze e P. Wick, «Micronized copper wood preservatives: An efficiency and potential health risk assessment for copper-based nanoparticles,» *Environmental Pollution,* vol. 200, pp. 126-132, 2015.

[4] C. Civardi, M. Schubert, A. Fey, P. Wick e F. W. Schwarze, «Micronized Copper Wood Preservatives: Efficacy of Ion, Nano, and Bulk Copper against the Brown Rot Fungus Rhodonia placenta,» *PloS one,* vol. 10, n. 11, 2015.

[5] European Institute for Wood Preservation, «The wood preservation industry,» [Online]. Available: http://www.wei-ieo.org/woodpreservation.html. [Consultato il giorno 2016 12 20].

[6] M. Pattanaik e S. K. Bhaumik, «Adsorption behaviour of polyvinyl pyrrolidone on oxide surfaces,» *Materials Letters,* vol. 44, n. 6, pp. 352-360, 2000.

[7] M.-A. Neouze e U. Schubert, «Surface modification and functionalization of metal and metal oxide nanoparticles by organic ligands,» *Monatshefte für Chemie-Chemical Monthly,* vol. 139, n. 3, pp. 183-195, 2008.

[8] H. L. Karlsson, P. Cronholm, J. Gustafsson e L. Möller, «Copper Oxide Nanoparticles Are Highly Toxic: A Comparison between Metal Oxide Nanoparticles and Carbon Nanotubes,» *Chemical Research in Toxicology,* vol. 21, n. 9, pp. 1726-1732, 2008.

[9] A. L. Costa, C. Galassi e R. Greenwood, «α-Alumina–H2O interface analysis by electroacoustic measurements,» *Journal of colloid and interface science,* vol. 212, n. 2, pp. 350-356, 1999.

[10] W. S. Cho, R. Duffin, F. Thielbeer, M. Bradley, I. L. Megson, W. MacNee, C. A. Poland, C. L. Tran and K. Donaldson, "Zeta Potential and Solubility to Toxic Ions as Mechanisms of Lung Inflammation Caused by Metal/Metal Oxide Nanoparticles," Toxicological Sciences, vol. 126, no. 2, pp. 469-477, 2012.

[11] European Commission - The Seventh Framework Programme, «Sanowork: Develop & identify a safe occupational exposure scenario,» [Online]. Available: http://www.safenano.org/research/sanowork/. [Consultato il giorno 2016 12 20].

[12] S. Patil, A. Sandberg, E. Heckert, W. Self e S. Seal, «Protein adsorption and cellular uptake of cerium oxide nanoparticles as a function of zeta potential,» *Biomaterials,* vol. 28, n. 31, pp. 4600-4607, 2007.

[13] L. S. Puah, R. Sedev, D. Fornasiero, J. Ralston e T. Blake, «Influence of surface charge on wetting kinetics,» *Langmuir,* vol. 26, n. 22, pp. 17218-17224, 2010.

[14] M. Ratoi, P. H. Hoet, A. Crossley e P. Dobson, «Impact of lung surfactant on wettability and cytotoxicity of nanoparticles,» RSC Advances, vol. 4, n. 39, pp. 20573-20581, 2014.

[15] M. L. Eggersdorfer e S. E. Pratsinis, «Agglomerates and aggregates of nanoparticles made in the gas phase,» Advanced Powder Technology, vol. 25, n. 1, pp. 71-90, 2014.

[16] M.-N. Croteau e S. N. Luoma, «Characterizing Dissolved Cu and Cd Uptake in Terms of the Biotic Ligand and Biodynamics Using Enriched Stable Isotopes,» *Environmental Science & Technology,* vol. 41, n. 9, pp. 3140-3145, 2007.

[17] K. V. Brix, A. J. Esbaugh e M. Grosell, «The toxicity and physiological effects of copper on the freshwater pulmonate snail, Lymnaea stagnalis,» *Comparative Biochemistry and Physiology Part C: Toxicology & Pharmacology,* vol. 154, n. 3, pp. 261-267, 2011.

3 SYNTHETIC IDENTITY

In this chapter are reported results referred to dry-state characterisation of pristine and modified samples in order to identify structural and surface properties and highlight differences between pristine and modified samples.

3.1 Electronic microscopy results

FE-SEM microscopies of pristine powder (Figure 3.1) show the presence of primary particles aggregates spheroidal above micrometre of diameter and this explains why it is difficult to produce starting suspensions with a good colloidal stability. Observing the surface of these particles more closely, it is possible to see the nanostructured surface: the primary particles, of about 20nm, are arranged to create a sponge-like structure with a high surface area.

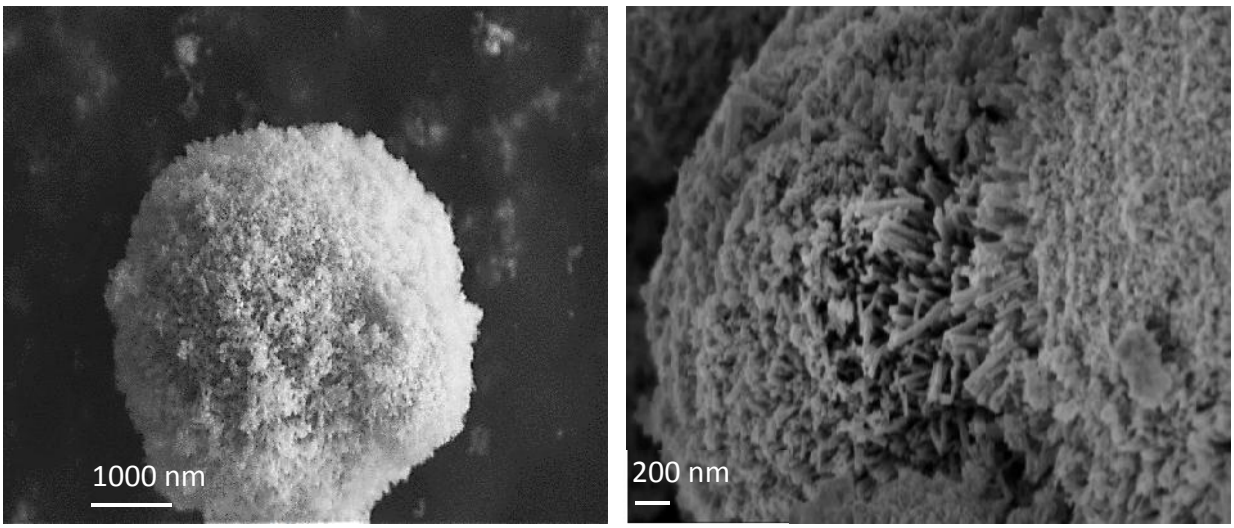

Figure 3.1 FE-SEM micrography of CuO NPs at different magnitude

The powder state of aggregation influences important properties such as surface area, reactivity and the dispersibility in wet media. Such property is crucial also because affects other risk relevant features such as powder dustiness and so the potential for nano-aerosolization in occupational nanomanufacturing settings [1]. For these reasons the control of agglomeration state and, in particular, the introduction of agglomeration steps that can decrease powder dustiness without affecting

nanoscale reactivity could represent a smart design solution for nanopowder processing.

Figure 3.2 and 3.3 show the morphology of the starting sol, after ball milling and after spray drying for CuO and CuO ascorbate powders.

Considering the unmodified CuO powder (Figure 3.2) it is possible to see that the material present itself in CuO_1 (pristine) and in CuO_24 (dried from suspension) as large aggregates, the ball milling treatment breaks those aggregates giving in CuO_91.1 a suspension of smaller, non-spherical, aggregates. The spray drying of the ball milled material gives again the spherical structure in CuO_96 that is maintained when the material is dispersed again in water suspension only by ultrasonic mixing as is the sample CuO_99.

Similar assumptions can be made for the modified CuO with sodium ascorbate, from right to left: the starting material with the addition of sodium ascorbate shows in CuO_78 the same aggregates even more adhering to each other; after ball milling the powder gives CuO_88.1 where the aggregates are broken into smaller fragments; after the spray drying of this sample in CuO_97 the larger spherical aggregates are reintroduced and the structure is maintained in CuO 100 after water suspension aided by ultrasonic mixing is produced.

From the analysis of re-dispersed powder based both on DLS (insert of Figure 3.2) and SEM-FEG images it seems that the suspension obtained after spray drying (CuO_99 and CuO_100) are very similar to the starting suspension (CuO_24): larger spherical aggregates are present together with a more dispersed nano-fraction, detected by DLS below 300nm.

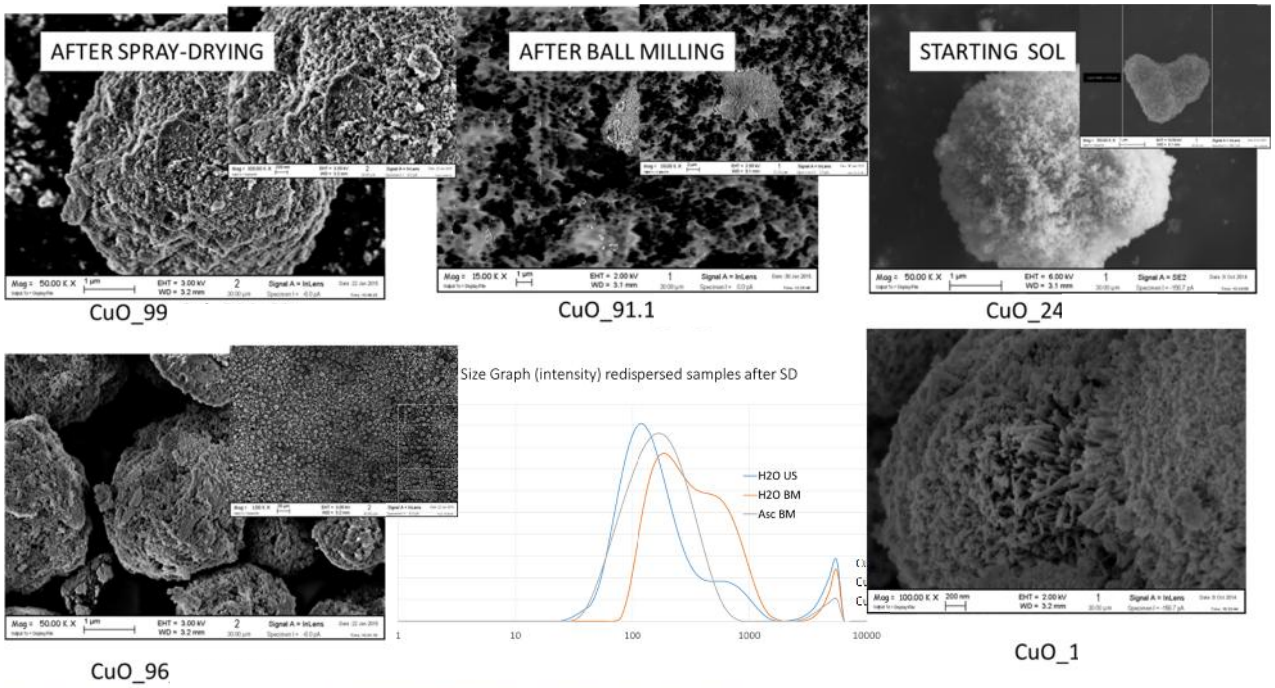

Figure 3.2_Starting sol, after ball milling and after spray-drying for CuO powder

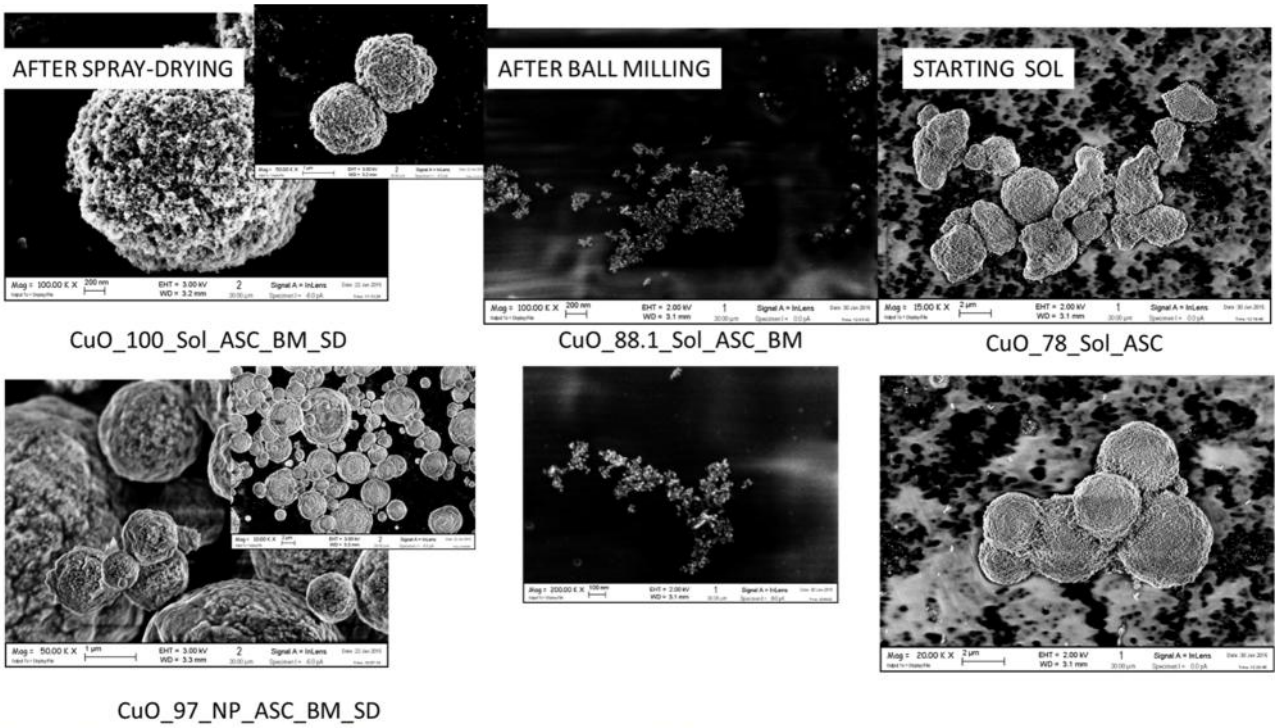

Figure 3.3_Starting sol, after ball milling and after spray-drying for CuO-ascorbate powder.

The STEM images were performed on samples aged three months, in particular on CuO pristine powder and on the ascorbate-modified (Figure 3.4). The analysis of the images evidenced the presence of primary nanoparticles with an average diameter of about 12±8 nm for the pristine sample in agreement with diameter observed by TEM on as synthesized powder (Figure 2.2). Ascorbate modified samples showed with aging an increased aggregation without significant changes in primary particle size (22±9 nm).

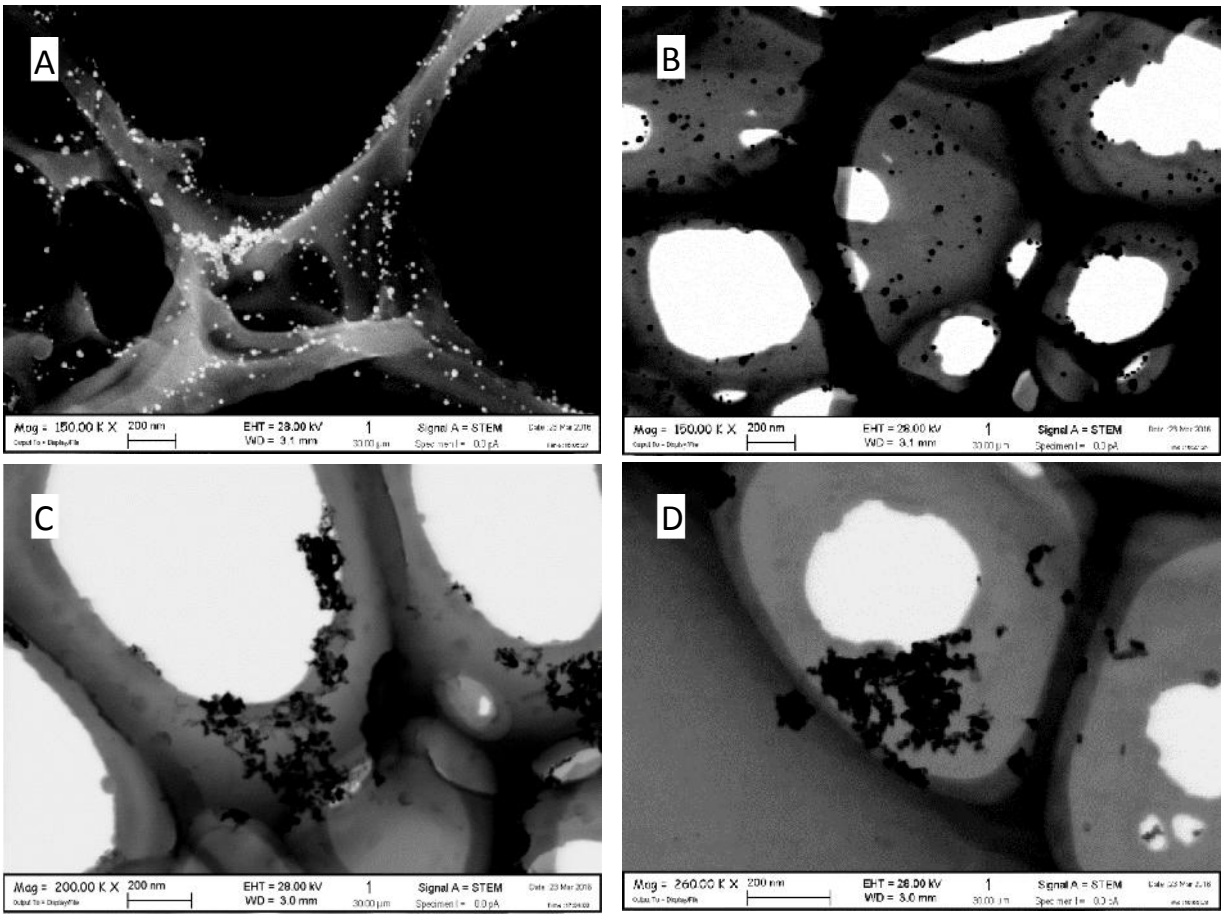

Figure 3.4_STEM images of Cu Pristine (A, B) and of Cu_105.8_ASC (C, D)

3.2 Coating efficency

3.2.1 Zeta potential titration results

Sodium citrate and PVP reached a plateau in Zeta potential trend after approximately 10% weight ratio between modifier and CuO mass; B-PEI showed a continuous upward trend for Zeta potential, in the examined concentration range, but displayed as well a plateau in mean particle size trend after reaching 10% modifier/CuO weight ratio (figure 3.5).

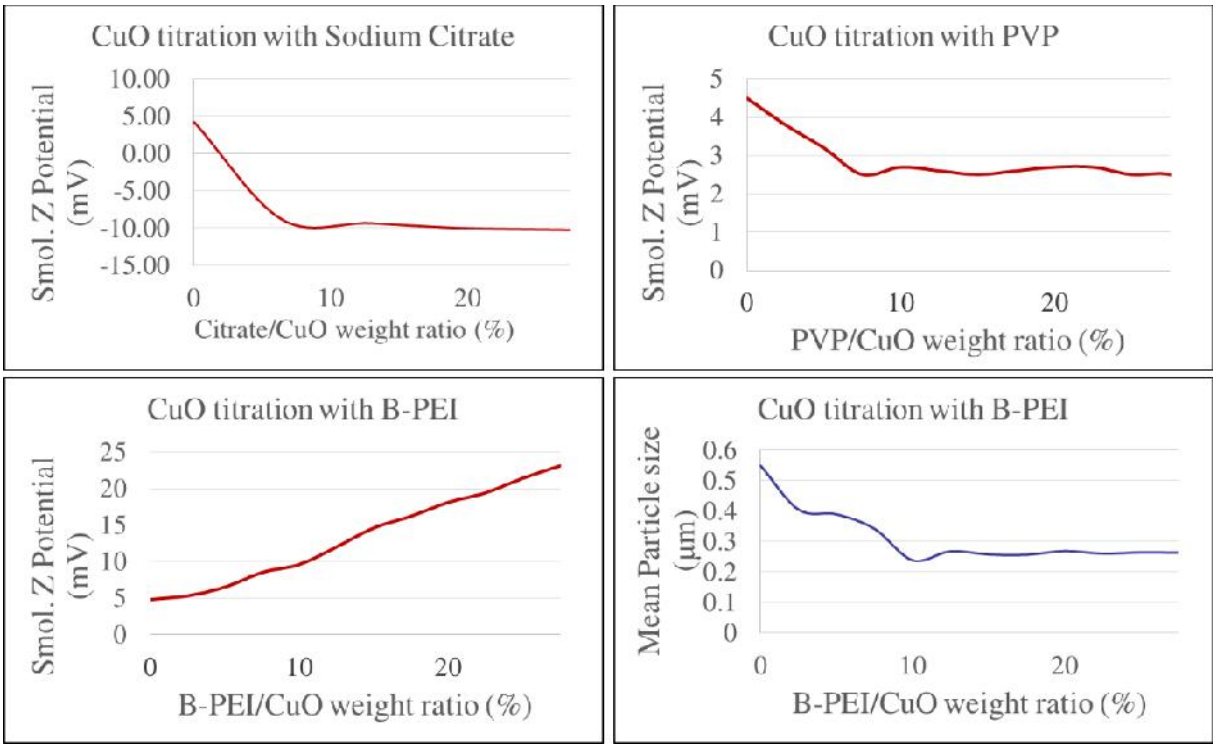

Figure 3.5_Results of titrations of CuO with different modifiers.
(a) Zeta potential Vs Sodium citrate, (b)Zeta potential Vs PVP, (c) Zeta potential Vs B-PEI, (d) PSD Vs B-PEI.

In the absence of a clear indication from Zeta potential, I examined the particle size profile (collected by the same instrument while measuring Zeta potential), identifying the best amount of modifier corresponding to the higher colloidal stabilization (lower mean particle size). Due to general indication provided by these preliminary results I chose 10% vs CuO mass as best amount of modifying agent and used the same amount also for ascorbate, since it was added to the study in a second stage of the research as promising candidate for the control of oxidative stress.

3.2.2 Thermogravimetric results

From thermogravimetric analysis results reported on Table 3.1, it is observed that CuO NPs dispersed in buffer phosphate are coated both by phosphate ions and by the coating agents. The pristine sample (CuO_24) showed the lowest weight loss whilst pristine sample dispersed in phosphate buffer (CuO_101) and modified samples showed a higher weight loss, due to the presence of the phosphate and of the coating agents adsorbed onto the surface. Likewise, the not ultrafiltered samples showed a higher weight loss compared to ultrafiltered ones where the modifier excess was removed.

Table 3.1_Thermogravimetric results achieved for CuO pristine and modified samples (filtered and not filtered).

		Phosphate + Coating agent		Coating Agent	
Sample	**Weight loss (%)**	**Adsorbed Amount (wt. %)**	**Total Amount (wt. %)**	**Adsorbed Amount (wt. %)**	**Total Amount (wt. %)**
CuO_24	2.6				
CuO_101 (UF)	3.5	5.6			
CuO_101 (NO UF)	4.2		9.5		
CuO_102 (UF)	4.7	2.2		1.3	
CuO_102 (NO UF)	8.0		5.6		4.6
CuO_103 (UF)	6.3	4.3		3.2	
CuO_103 (NO UF)	10.1		8.8		7.8
CuO 104 (UF)	8.6	6.9		5.8	
CuO 104 (NO UF)	11.9		10.7		9.7
CuO 105 (UF)	4.7	2.2		1.3	
CuO 105 (NO UF)	9.2		6.8		5.9

Considering the results of ultrafiltered samples, it is observed that citrate and ascorbate had the lowest value, around 1.3% whilst PEI showed the highest value, around 5.8%. An intermediate value (3.2%) was observed by PVP coating agent. Probably, the negative charge of citrate and ascorbate adversely affects the coating properties on negatively charged CuO NPs in buffer phosphate, with a resulting adsorbed capacity of 27 % for CIT and 21% for ASC. An intermediate adsorbed capacity was estimated for PVP (42 %). On the other hand, the positive charge of PEI (adsorbed capacity ≈ 60%) promote its adsorption on negatively charged CuO NPs.

3.3 X-Ray diffraction results

XRD results confirmed the oxide structures for all the analysed samples, corresponding to the crystalline phase of CuO (JPCDS 65-2309, space group C2/c) and showing that the addition of the different chelating agents did not change the crystalline phase of the material (Figure 3.6, 3.7, 3.8).

For each analysed modified material, the XRD pattern has been collected also for the pristine CuO pattern and from direct comparison it is possible to see that the modified materials peaks are matching the ones from pristine CuO.

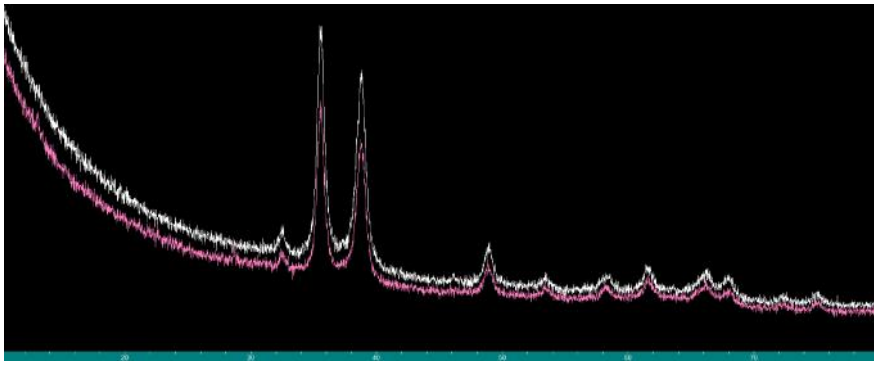

Figure 3.6_XRD pattern of Pristine CuO (pink line) and CuO_102.8_CIT (white line)

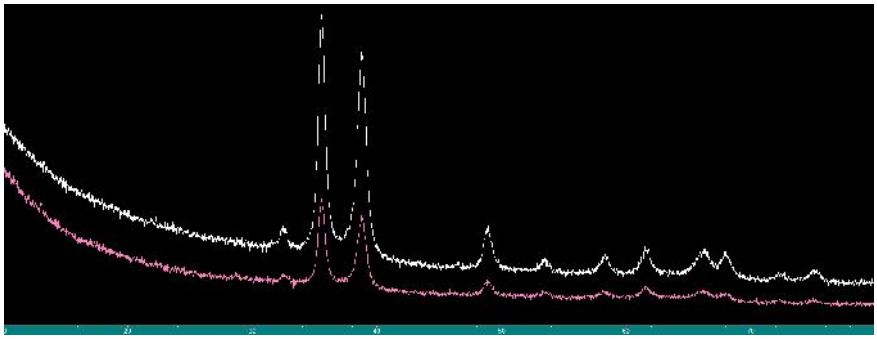

Figure 3.7_XRD pattern of Pristine CuO (pink line) and CuO_104.8_PEI (white line)

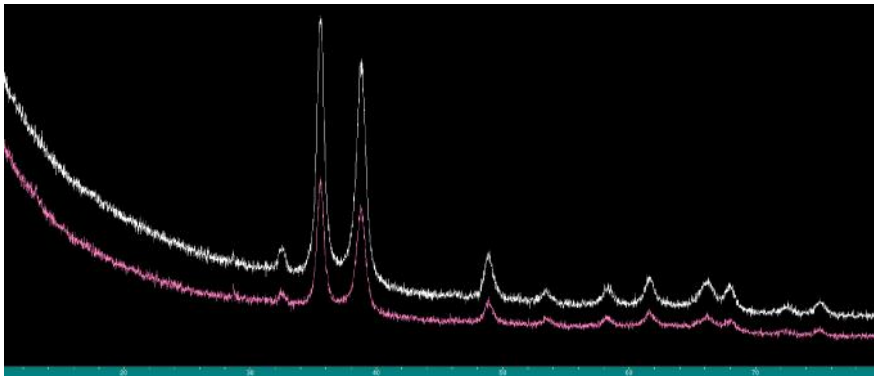

Figure 3.8_XRD pattern of Pristine CuO (pink line) and CuO_105.8_ASC (white line)

3.4 References

[1] L. Reijnders, «Human health hazards of persistent inorganic and carbon nanoparticles,» *Journal of Materials Science,* vol. 47, n. 13, pp. 5061-5073, 2012.

4 EXPOSURE IDENTITY

4.1 Isoelectric point results

Zeta potential values as a function of pH were recorded and the isoelectric point calculated at pH 10.3 (Figure 4.1). Within the pH range tested, values for the CuO NPs are between +30 mV and -30 mV, under limit of theoretical electrostatic stabilisation from DLVO theory.

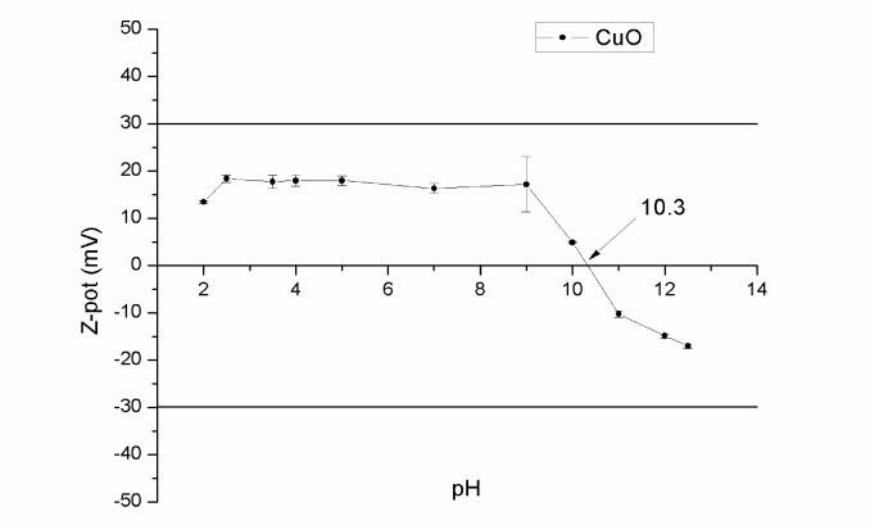

Figure 4.1_measured Zeta potential for samples with different pH, i.e.p. calculated at 10.3

4.2 Zeta potential results

4.2.1 Pristine CuO NPs

Table 4.1 shows Zeta potential results measured in ultrapure water and buffers for the pristine stock suspensions.

Table 4.1_Zeta potential characterization of pristine stock suspensions

Stock medium	Dilution medium	Sample	Description	Zeta Potential (mV)
H_2O	Ultrapure H_2O	CuO_24	US mixing	+34.9 ± 0.9
		CuO_91.5	Ball milling	+35.0 ± 0.3
Borate buffer		CuO_92	US mixing	-32.3 ± 1.0
		CuO_94	Ball milling	-4.8 ± 1.0
Phosphate buffer		CuO_106	US mixing	-26.6 ± 1.0
		CuO_101	Ball milling	-9.1 ± 0.4
	AFW	CuO_101	Ball milling	- 3.5 ± 0.4
	AMW			+7.6 ± 0.4
	MEM			-10.1 ± 0.5
	DMEM			-8.2 ± 0.4

Measured Zeta potential of biological media (based on suspended macromolecules) was -9.9 ± 0.7 for MEM and -10.6 ± 0.8 for DMEM.

The first important result found was the reverse of Zeta potential sign, comparing samples prepared in water with the ones prepared in buffer solutions. This was expected considering the specific adsorption of borate or phosphate oxyanions. The significant change of Zeta potential before and after the ball milling treatment, only for samples prepared in anionic buffer suspensions, can be justified considering the disaggregation occurred during ball milling with generation of free surface, not compensated by borate and phosphate ions adsorption. The increase of ionic strength in artificial fresh water and artificial marine water, due to the presence of Mg^{2+} and Ca^{2+} cations induced a colloidal destabilisation as shown by the decrease of Zeta potential and, in the case of artificial marine water (AMW), by the crossing of the isoelectric point. Sample diluted in biological media displays similar Zeta potential values that are close to values measured for media without NPs. This behaviour was

expected and is explained as the effect of amino acids excess that forms a bio-corona surrounding NPs surface.

4.2.2 Modified NPs

A complete wet state characterization of the modified samples was performed to verify the effects of surface coating on colloidal properties.

Zeta potential values of samples dispersed in borate buffer (stock suspension) and diluted in water before and after mechanical grinding treatment (ball milling) are reported in table 4.2.

Table 4.2_ Zeta Potential values of modified samples diluted in water, before and after ball milling treatment

Stock medium	Dilution medium	Modifying agent	Sample	Description	Zeta Potential (mV)
Borate buffer	Ultrapure H_2O	None	CuO_92	US mixing	-32.3 ± 1.0
			CuO_94	Ball milling	-4.8 ± 1.0
		CIT	CuO_33	US mixing	-37.2 ± 1.0
			CuO_53	Ball milling	-32.8 ± 1.0
		PVP	CuO_38	US mixing	-0.2 ± 1.0
			CuO_63	Ball milling	-10.2 ± 1.0
		B-PEI	CuO_43	US mixing	+33.9 ± 1.0
			CuO_73	Ball milling	+39.1± 1.0
		ASC	CuO_78	US mixing	- 30.2 ± 1.0
			CuO_88	Ball milling	- 35.6 ± 1.0
Phosphate buffer		None	CuO_101	Ball milling	-9.1 ± 0.4
		CIT	CuO_102		-18.0 ± 0.3
		PVP	CuO_103		-8.1 ± 2.3
		B-PEI	CuO_104		+28.3 ± 0.7
		ASC	CuO_105		-17.4 ± 0.3

The negative Zeta potential of pristine NPs due to adsorbed borate is increased in the presence of negative agents (citrate, ascorbate) if referred to ball-milled samples. Data are close to neutrality for neutral agent (PVP) and positive for positive modifier (PEI). This is what was anticipated and confirms the formation of the desired external layer on the NPs. Zeta potential of modified NPs diluted in environmental media is shown in table 4.3 (AFW) and table 4.4 (AMW).

Table 4.3_Zeta potential values for pristine and modified CuO NPs diluted in AFW

Stock medium	Dilution medium	Modifying agent	Sample	Zeta Potential (mV)
Phosphate buffer	AFW	None	CuO_101	-3.5 ± 0.4
		CIT	CuO_102	+3.6 ± 0.4
		PVP	CuO_103	+1.6 ± 0.3
		B-PEI	CuO_104	+20.9 ± 0.9
		ASC	CuO_105	-8.1 ± 0.4

Increased solution ionic strength (salinity), explains the measured Zeta potential values closer to neutrality; overall electric field screening by ions dissolved in the medium (Ca^{2+} and Mg^{2+}) disrupts the surface potential repulsion, promoting aggregation.

Table 4.4_Zeta potential values for pristine and modified CuO NPs diluted in AMW

Stock medium	Dilution medium	Modifying agent	Sample	Zeta Potential (mV)
Phosphate buffer	AMW	None	CuO_101	+ 7.6 ± 0.4
		CIT	CuO_102	+4.5 ± 0.7
		PVP	CuO_103	+6.5 ± 1.5
		B-PEI	CuO_104	+10.1 ± 1.1
		ASC	CuO_105	+2.7 ± 0.6

In AMW the total salinity and composition resulted so high that Zeta potential values were raised into positive values, crossing the i.e.p. for pristine and negatively charged NPs (CIT, ASC).

In biological media (MEM and DMEM), the levelling effect showed for pristine samples was confirmed and no difference was detected comparing different modified samples that all showed values coherent with Zeta potential of media alone (Table 4.5).

Table 4.5_Zeta potential values for pristine and modified CuO NPs dispersed in biological media

Stock medium	Modifying agent	Sample	Zeta Potential (mV)	
			Diluted in MEM	Diluted in DMEM
Phosphate buffer	None	CuO_101	-10.1 ± 0.5	-8.2 ± 0.4
	CIT	CuO_102	-10.5 ± 0.2	-9.7 ± 0.6
	PVP	CuO_103	-10.1 ± 0.4	- 9.4 ± 0.8
	B-PEI	CuO_104	-10.5 ± 0.9	-10.1 ± 0.7
	ASC	CuO_105	-9.5 ± 0.2	-9.2 ± 0.2

4.2.3 Effects of aging on CuO NPs colloidal stability

In order to evaluate the aging effects on the CuO suspensions, a series of characterizations was performed on both fresh and aged samples (after 3 months) prepared in buffer phosphate suspensions.

Zeta potential data referred to fresh and aged working suspensions (stock suspension prepared in buffer phosphate and diluted in water) are listed in Table 4.6. The fresh samples showed values coherent with the charge given by the coating agent, as measured for buffer borate phosphate suspensions (Table 4.2). The aging time leads to a reduction of the colloidal stability for the pristine sample, consistent with the visual observation, and proved by the considerable reduction of Zeta potential, till values close to zero. This is due to the weak interactions between NPs surfaces and the phosphate ions that take the place of the coating agents. A similar behaviour is noted also for the NPs modified by sodium ascorbate; since this modifier can be affected by oxidation, turning the suspensions to brown in few hours. I supposed that

the Zeta potential change is a result of modifier exhaustion over time. Positive PEI and negative CIT preserved initial Zeta potential values, resulting as the most suitable coating agents for ensuring the long-term stability.

Table 4.6_Zeta potential data of fresh and aged CuO samples.

Sample	Zeta Potential (mV)	
	FRESH	AGED
CuO_101	-31.3 ± 0.6	-2.3 ± 0.5
CuO_102	-36.5 ± 0.5	-35.0 ± 0.6
CuO_104	+13.7 ± 0.6	+14.7 ± 0.5
CuO_105	-35.7 ± 1.5	-2.0 ± 1.5

4.3 Particle size distribution results

4.3.1 Pristine CuO NPs

Table 4.7 shows results of PSD of pristine samples prepared in water or buffers and diluted in different media. Comparing primary particle size, as reported by providers, with measured hydrodynamic mean diameters, points out the agglomerated/aggregated nature of powders when dispersed in water. It should be noted that the AAN value indicates good dispersions when is less than 100.

Table 4.7_Preliminary wet state characterization results

Stock medium	Dilution medium	Sample	Description	DLS PSD (nm)	Average agglomeration number (AAN)
H_2O	Ultrapure H_2O	CuO_24	US mixing	330 ± 19	3791
		CuO_91.5	Ball milling	301 ± 5	2877
Borate buffer		CuO_92	US mixing	1236 ± 47	199187
		CuO_94	Ball milling	3300 ± 65	3790943
Phosphate buffer		CuO_106	US mixing	226 ± 80	1218
		CuO_101	Ball milling	2050 ± 350	908797
	AFW	CuO_101	Ball milling	4244 ± 45	8063648
	AMW			4279 ± 173	8264799
	MEM			47 ± 6	11
	DMEM			55 ± 16	18

Average measured PSD of biological media (based on suspended macromolecules) was 20.8 ± 0.5 nm for MEM and 17.4 ± 0.3 nm for DMEM.

4.3.2 Ball milling effect

The suspensions prepared in water and in buffered systems were ball milled at two different times, 24h and 95h, in order to see if the mechanical force of ball milling treatment could be enough to break aggregates and to disperse the NPs, such experiment also simulated weak forces that will act on the particles after the environmental release, representing the natural wearing. After the experiments, the particle size distribution of the milled powder was analysed, the results obtained, compared with the NPs dispersed only by ultrasonic mixing, are reported in figure 4.2.

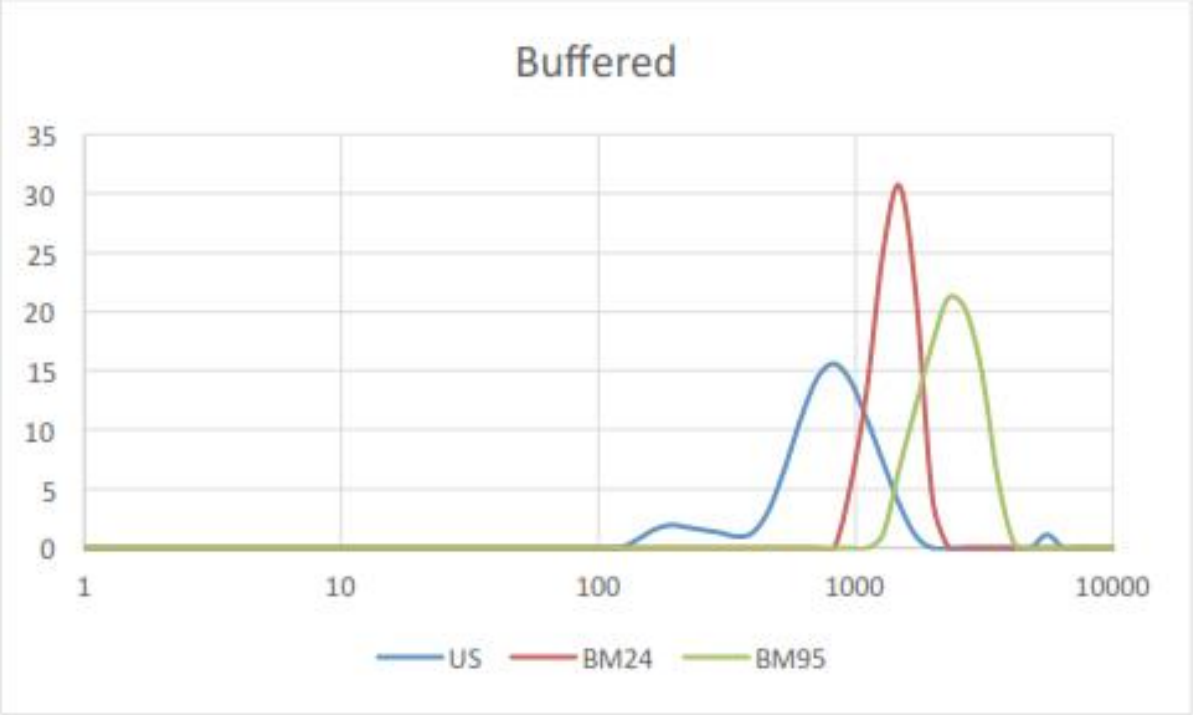

Figure 4.2_PSD resulted from DLS analysis of pristine sample ultrasonicated (US) and after ball milling treatment (BM) for different times

From the results, the wet ball milling treatment does not seem to have any disaggregation effect: milled samples present even more large aggregates, nevertheless the loss of spherical shape due to milling treatment may affect the quality of the instrumental analysis and explain such results. We hypothesized that initial aggregates were in a stable spherical conformation, the disaggregation effect of mechanical milling breaks those aggregates, releasing free particles that can promote a further aggregation of the fragments. The loss of spherical shape for the aggregates and the formation of dendrimeric structures are confirmed by FE-SEM observations.

4.3.3 Modified NPs

Particle size characterization in buffer borate suspensions were performed both before and after disaggregation treatment (ball milling), results are showed in table 4.8.

Table 4.8_ DLS mean diameter and AAN of modified samples diluted in water, before and after ball milling treatment

Stock medium	Modifying agent	Sample	Description	Mean diam. (nm)	AAN
Borate buffer	None	CuO_92	US mixing	1236 ± 47	199187
		CuO_94	Ball milling	3300 ± 65	3790943
	CIT	CuO_33	US mixing	1759 ± 348	574120
		CuO_53	Ball milling	177 ± 35	584
	PVP	CuO_38	US mixing	1579 ± 299	415290
		CuO_63	Ball milling	2900 ± 393	2572761
	B-PEI	CuO_43	US mixing	1781 ± 312	595932
		CuO_73	Ball milling	179 ± 44	605
	ASC	CuO_78	US mixing	350 ± 71	4522
		CuO_88	Ball milling	169 ± 37	509
Phosphate buffer	None	CuO_101	Ball milling	2052 ± 347	911460
	CIT	CuO_102		313 ± 8	3235
	PVP	CuO_103		797 ± 24	53405
	B-PEI	CuO_104		383 ± 22	5927
	ASC	CuO_105		109 ± 2	137

These experiments showed that PVP does not improve colloidal stabilization, leading to larger aggregates after ball milling treatment. Otherwise the ball milling treatment is effective in the case of ionic modifying agents, confirming the synergic action between mechanical grinding and electrostatic repulsion of ionic coatings. The citrate modified sample after disaggregation resulted well dispersed, with a thousand times lower AAN. Ascorbate agent seems the most effective in terms of dispersion capacity, as confirmed by the high fraction of submicrometric particles also present in the sample pre-ball milling (around 350nm). The results of B-PEI modified samples confirmed that also cationic dispersants are able to disaggregate particles if coupled with ball milling mechanical treatment.

The PSD has been measured studying the evolution of the system in the life cycle, as previously showed for Zeta potential determination. Results for environmental media are summarized in the following tables 4.9 (AFW) and 4.10 (AMW).

Table 4.9_PSD values for pristine and modified CuO NPs diluted in AFW

Stock medium	Dilution medium	Modifying agent	Sample	DLS PSD (nm)
Phosphate buffer	AFW	None	CuO_101	1663 ± 210
		CIT	CuO_102	1050 ± 16
		PVP	CuO_103	1159 ± 256
		B-PEI	CuO_104	675 ± 199
		ASC	CuO_105	1293 ± 278

As discussed above, the high solution ionic strength (salinity) leads to Zeta potential attenuation and promotes the aggregation of NPs. Measured PSD showed the expected aggregation for every tested system, pristine and modified.

Table 4.10_ PSD values for pristine and modified CuO NPs diluted in AMW

Stock medium	Dilution medium	Modifying agent	Sample	DLS PSD (nm)
Phosphate buffer	AMW	None	CuO_101	1281 ± 393
		CIT	CuO_102	1062 ± 159
		PVP	CuO_103	1661 ± 68580
		B-PEI	CuO_104	1281 ± 1.1
		ASC	CuO_105	1234 ± 25

The aggregation induced by salinity is clearly stronger in AMW, for this medium there is no colloidal stability, the aggregation rapidly occurs as showed by measured particle size distributions and the NPs settle from the suspensions.

The effect of amino acids smoothed the differences between pristine and modified samples in biological media, table 4.11. The formation of protein bio-corona around NPs greatly improved the dispersion of the particles, such stabilization may be explained as a combination of amino acids surface adsorption on NPs and sequestration of copper cations, suggesting that in biological media the solubility of the studied material should be higher as well.

Table 4.11_Zeta potential values for pristine and modified CuO NPs diluted in biological media

Stock medium	Modifying agent	Sample	DLS PSD (nm)	
			Diluted in MEM	Diluted in DMEM
Phosphate buffer	None	CuO_101	47.2 ± 6	55.1 ± 16
	CIT	CuO_102	89.5 ± 5	37.4 ± 2
	PVP	CuO_103	43.8 ± 2	52.9 ± 25
	B-PEI	CuO_104	46.1 ± 4	44.6 ± 14
	ASC	CuO_105	51.6 ± 4	72.8 ± 21

4.3.4 Aging evaluation

Table 4.12 shows the average hydrodynamic diameters collected on both fresh and aged suspensions.

Table 4.12_Size data (Zeta-average) of fresh samples and aged samples

Sample	DLS PSD (nm)	
	FRESH	AGED
CuO_101	1093 ± 50	1575 ± 188
CuO_102	368 ± 10	438 ± 70
CuO_104	247 ± 14	842 ± 57
CuO_105	122 ± 1.4	ND*

ND * = not determined due to fast sedimentation

Data collected from fresh samples confirmed the anticipated effects of the surface modifiers as already observed in the previous section 4.2.4. The samples aged 3 months produced higher agglomeration, clearly observed by the increase of the hydrodynamic diameter. In order to allow the DLS measurement and to assess the size distribution of the agglomerates after aging, an ultrasound treatment was applied. The data collected showed that ascorbate-modified sample, during the storage, loose its colloidal stability, resulting in the precipitation of large aggregates; in the other samples, the visible sediment was easily dispersed, giving measured values roughly comparable with fresh samples. B-PEI, seemed to be the most effective additive for the long term colloidal stability. On the contrary, the ascorbate was greatly effective on the fresh sample, but not suitable for the long-term storage.

4.4 Further wet state characterisation

4.4.1 Aging effect on pH

The pH values, measured both on aged and fresh samples, are listed in Table 4.13.

Table 4.13_pH of fresh stock and working suspensions and aged stock and working suspensions, diluted in ultrapure water

Sample	pH	
	FRESH	AGED
CuO_101	9.4	9.1
CuO_102	8.7	8.6
CuO_104	10.1	8.4
CuO_105	7.8	7.8

Despite the presence of phosphate buffer, the stock suspensions showed higher values of pH than the buffer (pH = 7.4). Our hypothesis is that the buffering mechanism is altered both by the interaction of the PO_4^{3-} ions with the CuO surface and by the precipitation of the insoluble copper phosphate $Cu_3(PO_4)_2$ salt. The data evidenced very close pH values for both aged and fresh suspensions, proving the chemical stability of these systems over the storage time. Only the B-PEI modified sample exhibited a marked pH variation during the storage, reaching values closer to the other samples, probably due to its initial interaction with the negative CuO/PO_4^{3-} surface that reaches stability (adsorption of the modifier) after longer periods.

4.5 Sedimentation velocity results

Figure 4.3 shows values of the average sedimentation velocity for pristine and modified CuO NPs dispersed in different media, revealing a correlation with the hydrodynamic diameter.

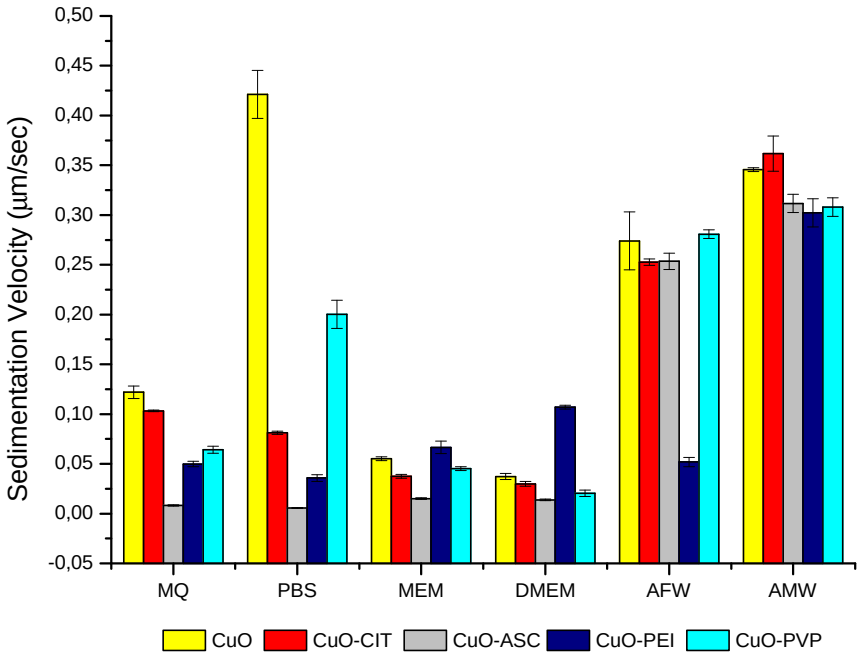

Figure 4.3_Average sedimentation velocity data for pristine and modified CuO NPs dispersed in different media

Sedimentation velocity distributions are reported in Figure 4.6. In general, it was confirmed that the modifying agents improved the colloidal stability of the dispersions, avoiding or decreasing the formation of CuO aggregates with respect to pristine CuO NPs. In particular, as far as ultrapure water and PBS media, the sedimentation velocity distribution decreased for all the modified suspensions compared to pristine CuO NPs. The sedimentation velocity rate in these two aqueous media followed the same rank observed for hydrodynamic diameter data in ultrapure water, in which pristine and CuO-PVP suspensions are less stable than CuO-CIT followed by CuO-PEI and CuO-ASC. The correlation between ASV and DLS data was also noticed for CuO-pristine and CuO-PVP dispersed in PBS, showing both the highest sedimentation velocity values and agglomeration rates. Surprisingly, CuO-

ASC dispersion revealed the lowest sedimentation velocity values in PBS but high average hydrodynamic diameter (> 1 µm). Taking into account the two different cell culture media (MEM and DMEM), the results from ASV and DLS suggest that proteins and amino acids enhance the stability of the dispersions, both for pristine as well as for modified CuO. The only exception is represented by slightly higher sedimentation velocity values of CuO-PEI than the other dispersions.

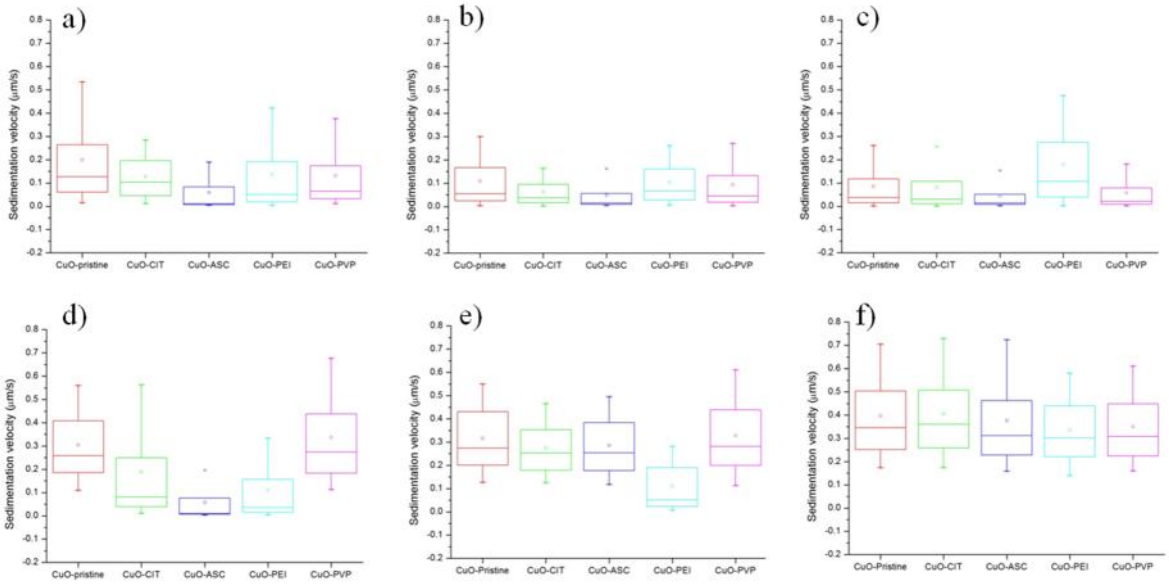

Figure 4.4_Sedimentation velocity distribution of pristine and modified CuO NPs dispersed in: a) Ultrapure water, b) MEM, c) DMEM, d) PBS e) AFW and f) AMW

However, a more precise analysis of the sedimentation rates can be achieved by considering instrument numerical data thorough their quartiles, using box plot as a graphical descriptive statistic (Fig. 4.4).

NPs dispersed in environmental media followed the same rank observed by DLS. An increase of instability was shown for all the samples both in AFW and AMW, except for CuO-PEI which showed an higher stability in AFW, resulting in agreement with hydrodynamic size and Zeta potential values.

5 HAZARD IDENTITY

5.1 Dissolution and solubility

After experimental confirmation that the proposed SbyD strategies have produced the expected modifications of the starting material (CHAPTER 3), the new NPs were observed in different media, simulating the environment that the material will cross through the life cycle. During these experiments, the evolution of the material colloidal stability was studied through assessment of the DLVO theory key parameters (average size and Zeta potential) (CHAPTER 4).

During the same experiments, it is also significant to study the solubility of the material both immediately after the introduction in the suspension (dissolution) and under equilibrium condition (solubility). The gathered information is essential to estimate the toxicological activity of the material and provides fundamental data for the interpretation of the successive toxicity tests.

5.1.1 Coating agents' activity

Solubility was evaluated for each proposed modifier in buffered pH suspensions by preparing five suspensions with modifier/CuO % weight ratio in the range between 2,4% and 12,2% and determining the dissolved fraction (figure 5.1). Sodium citrate showed the highest impact on copper solubility, reaching about 1 to 1 ratio (50% of copper dissolved) at a citrate to copper oxide ratio of 10%. PVP, on the contrary, showed no contribution at all, the dissolved fraction was under the detection limit at each concentration. PEI showed some effect but not as significant as that of citrate.

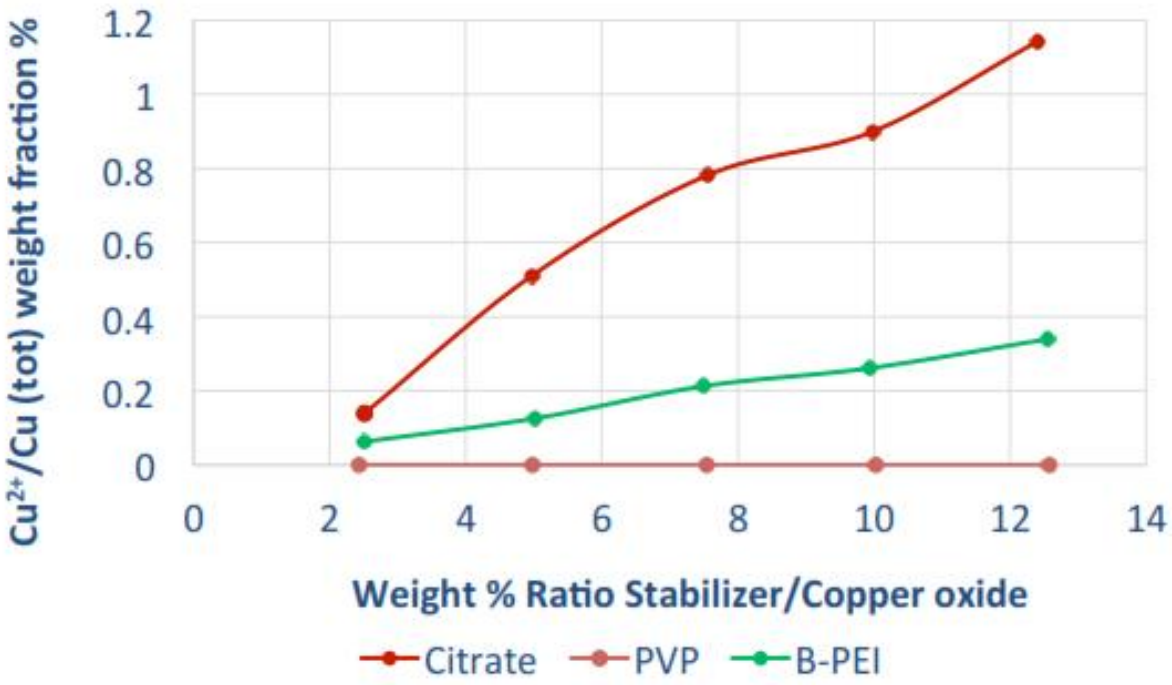

Figure 5.1_effect of modifiers concentration on solubility in pH buffered suspensions

The direct comparison between anionic modifiers shows a big difference between sodium citrate and ascorbate, with the latter having no visible effects on solubility (figure 5.2) while maintaining similar or better results in terms of disaggregation and colloidal stabilization.

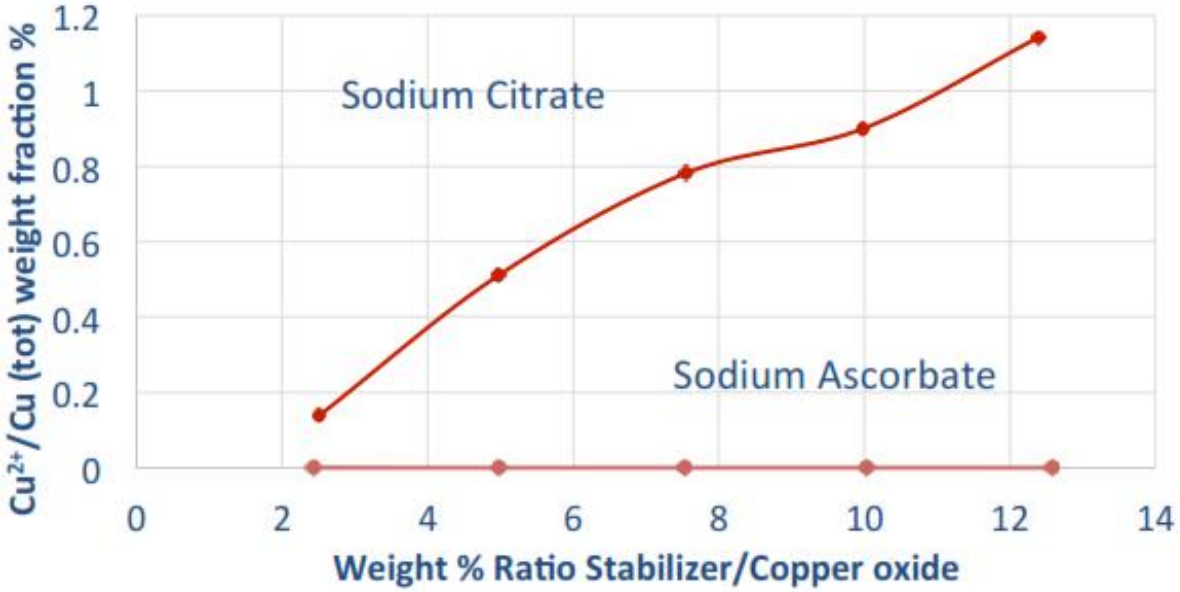

Figure 5.2_Comparison of sodium citrate and sodium ascorbate effect on CuO solubility in buffered suspensions

5.1.2 Testing media activity

Tested media:

For the third stage (eco-tox activity) characterization, the experiments were done in the benchmark condition and in the media that represent environmental scenario or cell culture dispersion. The selected test media were:

- Ultrapure water (laboratory condition)
- Artificial Freshwater OECD 203 (environmental medium)
- Artificial Marine water (environmental medium)
- MEM (cell culture medium)
- DMEM (cell culture medium)

Environmental medium results:

AFW

As showed in the ENPs characterization after modification, the ionic modifiers exercise an influence on the solidity of CuO and this influence is showed also in environmental medium solubility assay (Table 5.1).

Table 5.1_Dissolution and solubility estimation for pristine and modified CuO NPs diluted in AFW

Modifier	Dissolution at 1h Cu^{2+} / Cu_{tot} (%)	Solubility at 24h Cu^{2+} / Cu_{tot} (%)
Pristine (CuO_101)	0	0,25
Citrate (CuO_102)	2,52	2,05
PVP (CuO_103)	0,02	0,1
B-PEI (CuO_104)	6,88	6,26
Ascorbate (CuO_105)	1,2	0,71

According to the determination of pH dependent solubility done during preliminary characterization of CuO NPs, pristine material after 24h of incubation shows compatibility with expected solubility, at phosphate buffered pH (7,4).

It is noteworthy that kinetic dissolution for ionic modified NPs exceed solubility equilibrium, reaching higher values after 1h than after 24h. PVP shows best performance according to solubility control.

AMW

The results obtained in artificial marine water point out an effect of the further increased salinity on the kinetic behaviour of particles. Almost no difference is noted for the pristine material and the neutral (PVP): poor solubility. Negative agents (citrate and ascorbate) show again the reprecipitation after 24 hours behaviour, with an overall slightly increased solubility. The positive material shows fast aggregation and precipitation, this reduces its mobility in the suspension and explain why it does not reach higher dissolution in the first hour compared to the solubility at 24 hours (Table 5.2).

Table 5.2_Dissolution and solubility estimation for pristine and modified CuO NPs diluted in AMW

Modifier	Dissolution at 1h Cu^{2+} / Cu_{tot} (%)	Solubility at 24h Cu^{2+} / Cu_{tot} (%)
Pristine (CuO_101)	0,04	0,27
Citrate (CuO_102)	3,07	2,41
PVP (CuO_103)	0,06	0,12
B-PEI (CuO_104)	3,15	7,41
Ascorbate (CuO_105)	4,48	0,67

Toxicological medium results:

Cell culture media are distinguished by elevated content of amino acids. These substances are capable of strong chelating effects, sequestering ions from the solution and rapidly influencing the overall solubility.

Experimental results in **MEM** and **DMEM** showed similar solubility between each NPs, suggesting that the chelating effects are far more influential than proposed surface modifications (Table 5.3).

Table 5.3_Dissolution and solubility estimation for pristine and modified CuO NPs diluted in DMEM

Modifier	Dissolution at 1h Cu^{2+} / Cu_{tot} (%)	Solubility at 24h Cu^{2+} / Cu_{tot} (%)
Pristine (CuO_101)	66.9	84.26
Citrate (CuO_102)	67.21	83.64
PVP (CuO_103)	61.97	82.51
B-PEI (CuO_104)	61.97	82.51
Ascorbate (CuO_105)	63.14	81.74

5.1.3 Electroanalytical methods

Anodic peaks were observed, and interpreted as due to stripping of Cu deposited onto the Au electrode during a previous cathodic run. The position E_{PEAK} of the peak on the potential axis, and its height I_{MAX}, were recorded and plotted vs. nominal Cu^{2+} concentration (Fig. 5.3). Monotonically increasing and reproducible peak height vs. [Cu^{2+}] calibration curves could thus be obtained in Aldrich D4031, DMEM and FBS-DMEM. As to Aldrich D8662, no reproducible correlations between Cu concentration and peak height could be observed.

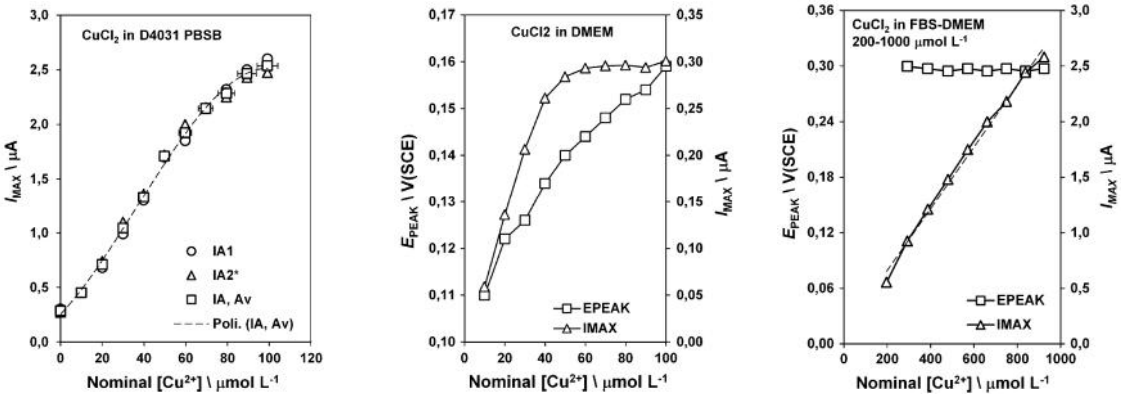

Figure 5.3_Calibration curves for Cu in D4031 PBSB (left), DMEM (centre), FBS-DMEM (right) [2]

The same deposition/stripping CV scans for calibration curves were then repeated, in the same media while adding CuO NPs as aqueous suspension (11% v/v of 1 g L^{-1} CuO in distilled water). The same anodic peaks appeared as those observed in $CuCl_2$-added media (Fig. 5.4).

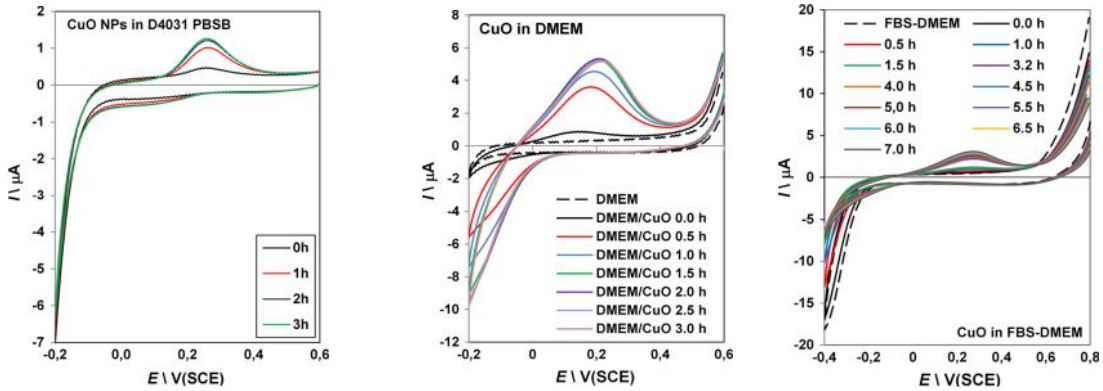

Figure 5.4_CV curves recorded in CuO-added D4031 PBSB, DMEM, and FBS-DMEM. The height of the anodic peak was observed to increase vs. time. CV curves recorded in CuCl2-added media were similar [2]

While all the above provides strong evidence of copper leaching in suspensions of CuO NPs in biological media at pH 7.4, minor differences were observed in the

electrochemical response of the CuO-NPs-added media with respect to that observed in $CuCl_2$-added media. The effect of adding glycine to $CuCl_2$-added D4013 PBSB was also studied, providing evidence that minor differences in the electrochemical behaviour of Cu in DMEM and FBS-DMEM (as compared to D4031 PBSB) could be explained by the presence of the amino acids present in DMEM and FBS-DMEM. Electroanalysis results thus far obtained strongly indicate that Cu leaching from CuO NPs is to be expected as a matter of course both in CuO NPs aqueous suspensions and suspensions in biological media, from a few percent of the total copper content in D4031 PBSB to 80% in FBS-DMEM over a few hours. Electroanalysis has been found to be helpful in monitoring and describing the chemical environment determined by the presence of CuO-NPs in the above media. In particular, Cu leaching has been observed at pH 7.4, questioning the stability of CuO NPs in buffered biological media. In the case of $CuCl_2$ in D8662 PBSB, electroanalysis provided strong evidence of some chemical mechanisms that were able to either subtract copper or inactivate it electrochemically, so that increasing amounts of added copper did not cause stronger CV copper features to be observed. The possible role of phosphate ions in this mechanism is currently being studied by means of CV at the platinum electrode. The trend of anodic features vs. time can be utilized to infer the kinetics of the leaching mechanism.

In conclusion, electroanalysis (an in situ, non-invasive and easily implemented technique) has evidenced both presence of Cu ions in the above media to which CuO NPs had been added, and the presence of mechanisms that seem to be able to electrochemically inactivate ionic copper. Such mechanisms seem to involve the role of phosphate ions, amino acids, and perhaps glucose, as evidenced by the comparison between results of $CuCl_2$ in D8662 PBSB and D4031 PBSB (Fig. 5.5), improving knowledge in terms of ion speciation.

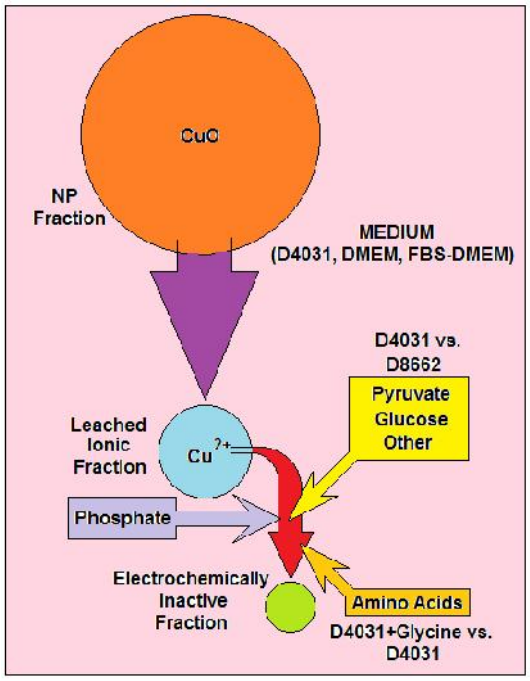

Figure 5.5_Schematic of the overall picture so far contributed by electroanalytical measurements to the mechanisms operating in CuO NPs-added biological media. Two main mechanisms are predicted: Cu leaching, and inactivation of leached Cu2+. The latter seems to be dependent on the presence or absence of medium components such as glucose, pyruvate, amino acids, and phosphate ion

5.2 Toxicological evaluation

Further investigations (in vitro and in vivo) are needed, giving a complete toxicological assay considering the type of exposures the product is going to encounter in its life cycle. If this stage demonstrate a sufficient reduction of risk related to the application of a coating agent, it will justify the strategy associated. This stage is required especially for the first strategies proposed: every produced data will be collected by other international projects to build predictive models. Such models will lead to reliable in silico assays whose results may be used to rapidly introduce others SbyD material into the market.

5.2.1 In vitro tests results

The pristine material was tested as benchmark: for the macrophage cell line (RAW264.7), the cytotoxicity assessment showed a high toxicity (BMD20 ≤100µg/ml) with the value of BMD20=25.50 µg/ml and EC50=40.97 µg/ml.
As an additional starting reference, the salt forms of Cu, CuCl2, was also tested using the same experimental setup: BMD20=55.60 µg/ml and EC50=63.91 µg/ml.
This displays that the CuO NPs are less safe than the completely dissolved copper.

The cytotoxic potential of the modified nanomaterial was then investigated using the same procedure applied on pristine CuO NPs. For the macrophage cell line (RAW264.7), the benchmark dose 20 (BMD20) was calculated in MEM and compared with pristine CuO, ball-milled and modified samples, leading to the following results (figure 5.6).

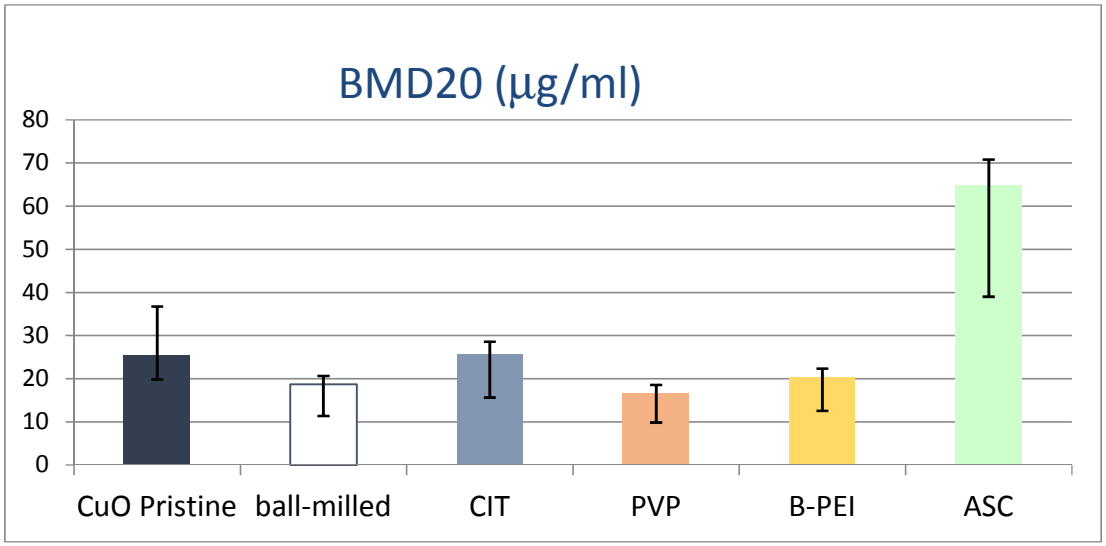

Figure 5.6_Cytotoxicity assays on macrophage cell line, results from SbyD modified and normal CuO NPs

It is evident in this case that Sodium Ascorbate modification has led to reduced toxicity of the final material, measured value (64.80 µg/ml) is even higher than the BMD20 measured for $CuCl_2$ (55.60µg/ml). The overall toxicity of the particles is still elevated since the value is lower than conventional threshold of 100µg/ml but outcomes point out a possible strategy to be explored for safer material (exploiting the ascorbate coating to probably achieve safer material). If the performance test demonstrates the activity improvement typical of nanomaterials, this result may suggest a strategy to obtain formulations safer and more efficient than standard bulk equivalents.

5.2.2 In vivo tests results

Table 5.4 summarize the LC50 results obtained in the preliminary evaluation of the materials, compared with the values measured for ball-milled CuO NPs and two of the proposed modified materials (B-PEI and ASC).

Table 5.4_Summary of LC50 values obtained in the L. stagnalis experiments

Material	LC50 96h
$CuSO_4$	5.5 µg L^{-1}
CuO NPs	2500 µg L^{-1}
Ball-milled CuO NPs	250 µg L^{-1}
B-PEI - CuO NPs	170 µg L^{-1}
Ascorbate - CuO NPs	ND

This test confirmed in vitro result: under the same conditions the Ascorbate coated NPs were loaded up to four time the concentration of the benchmark material (pristine CuO NPs) without measuring any toxic effect.

5.3 References

[2] C. Baldisserri e A. L. Costa, «Electrochemical detection of copper ions leached from CuO nanoparticles in saline buffers and biological media using a gold wire working electrode,» *Journal of Nanoparticle Research,* vol. 18, n. 4, 2016.

6 JUSTIFICATION OF SbyD SOLUTIONS

6.1 Testing strategy

In this study, I proposed a 4-level procedure to formulate and validate innovative SbyD that was:

1. Deep material analysis
2. Determination of key relevant properties modification (and verification)
3. Outcomes of the modification via toxicological evaluation
4. Final validation of safer procedures by performance tests

CuO NPs was selected for its intrinsic high toxicity and because it was already part of industrial manufacturing designed for the consumer products. The development of this project allowed to understand the toxic behaviour of copper oxide nanoparticles by observation of the key relevant properties of the dispersed material (solubility) in different media, in particular surface water (environment) or biological fluids (health).

A promising new approach is emerged from the proposed strategies; further industrial design may lead to the substitution of the original process with a safer one obtained with the resulted protocols, including therefore the wet grinding step with antioxidants in solution.

6.2 Performance evaluation

Overall results highlight the importance and necessity of further long term toxicological experiments and performance, in particular to evaluate chronic exposure to ENPs, environmental media substances effects [1] and assure nanotechnology sustainability.

6.2.1 Unmodified material performance

The nano-CuO synthesized by PlasmaChem was added to a high-gloss acrylic paint serving as a wood coating with an anticipated antimicrobial activity. The white base colour (acryl_FOR) is very similar to standards already described earlier in a publication from BASF [2]. Due to the addition of the CuO NPs, the acrylic paint is deteriorated to grey, but still allows half-shade colour adjustment by colouristic pigments.

A first formulation (CuO_acryl_FOR) according to a well-established dispersion method for paints resulted in an insufficient quality due to a drastic aggregation of the CuO (figure 6.1).

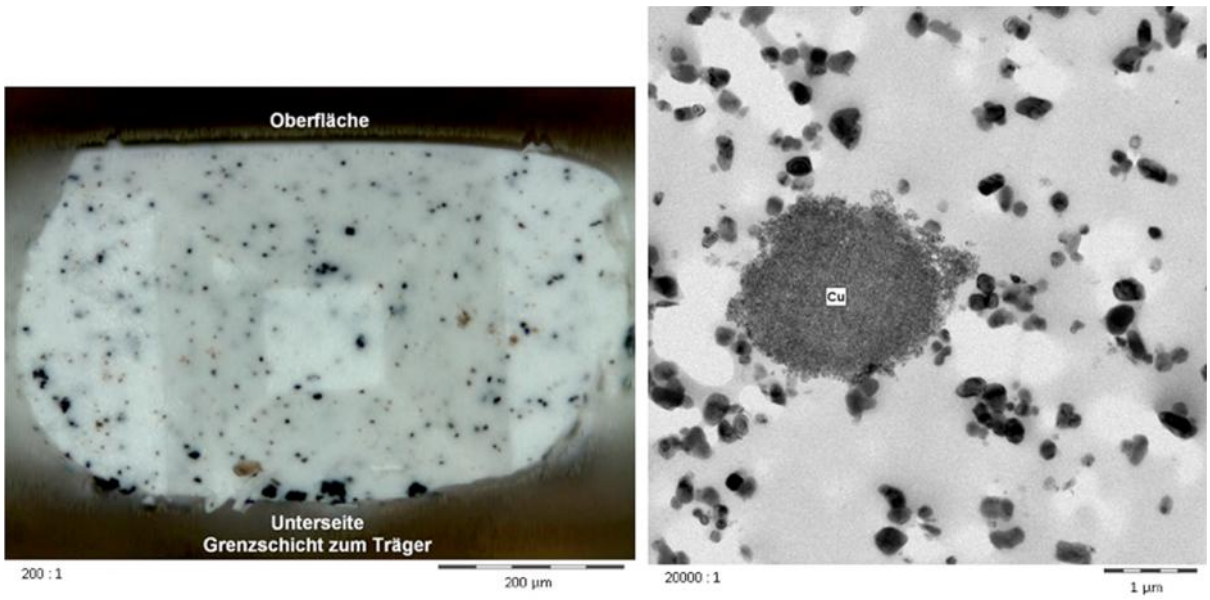

Figure 6.1_First formulation of CuO-based paint, agglomerated CuO (optical microscopy, left and TEM, right)

BASF provided the results of the wood degradation tests [3] (Table 6.1). The tests measure the loss of mass after 16 weeks exposition of pine wood blocks (2.5 x 2.5 x 1 cm^3) to coniophora puteana 62 (non Cu-tolerant fungus). Wood blocks are coated with CuO_acryl_FOR and acryl_FOR (negative control) and the results are compare to uncoated wood-blocks.

Table 6.1_Wood degradation tests

	CuO_acryl_FOR	acryl_FOR	Uncoated wood
Degradation (wt.%)	6%	10%	18%

6.2.2 Modified material performance

Since proposed strategy provided a promising SbyD modified material that resulted less toxic from in vitro and in vivo studies, the production of an alternative commercial formulation containing this nanomaterial is strongly suggested.

However, preliminary test from the manufacturer resulted in a decreased compatibility. While the initial material formulation was tuned for best performance (figure 6.2), producing fine dispersed Cu NPs in the commercial formulation (figure 6.2).

Figure 6.2_Optical microscopy comparison: first formulation of CuO-based paint (left) and after process optimization (right)

The Ascorbate-CuO NPs still require similar process optimization (figure 6.3) in order to enhance compatibility and reach original paint performances:

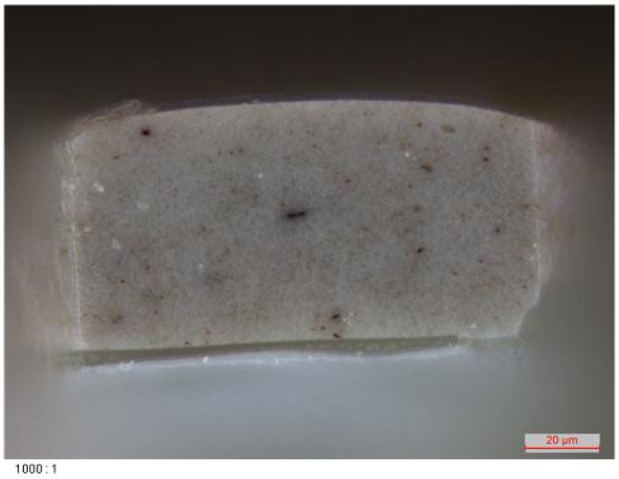

Figure 6.3_Optical microscopy comparison: first formulation of SbyD modified CuO NPs-based paint

6.3 References

[1] A. Pradhan, P. Geraldes, S. Seena, C. Pascoal e F. Cássio, «Humic acid can mitigate the toxicity of small copper oxide nanoparticles to microbial decomposers and leaf decomposition in streams,» *Freshwater Biology,* vol. 61, n. 12, pp. 2197-2210, 2016.

[2] F. Tiarks, T. Frechen, S. Kirsch, J. Leuninger, M. Melan, A. Pfau, F. Richter, B. Schuler e C. L. Zhao, «Formulation effects on the distribution of pigment particles in paints,» Progress in Organic Coatings, vol. 48, n. 2, pp. 140-152, 2003.

[3] WOOD PRESERVATIVES - TEST METHOD FOR DETERMINING THE PROTECTIVE EFFECTIVENESS AGAINST WOOD DESTROYING BASIDIOMYCETES - DETERMINATION OF THE TOXIC VALUES, DIN EN 113, 1996.

7 CONCLUSIONS

7.1 Main results

Global efforts towards nanotoxicology assessment are still slowed by the lack of multidisciplinary labours: the partnership forged with the different European research groups allowed to obtain relevant results in a relatively short time range, building the structure required to improve data collection and experimentation in the future.

Introduction and justification of safer by molecular design (SbyD) solutions have been made focusing this work on commercial CuO NPs. In order to achieve improved sustainability of nano-enabled commercial products, possible SbyD strategies were proposed according to the material main HSE issues, the candidate strategies were applied and their effect was studied to verify results on toxicity and risks related properties. Between the four investigated remediation strategies, involving organic coating of NPs by self-assembling procedure in a single step procedure, one appeared to be promising from the preliminary toxicological assessment.

Consequently, the multi-step procedure proposed to introduce and justify SbyD solutions for the reduction of (eco)-tox potential and preservation of final performances proved to be effective. The recognized fundamental steps required to validate and assess the differences produced by the modifications on the materials were:

- Level 1) Development and application of modification strategies, evaluating possible method to apply them in order to influence toxicological pathways;
- Level 2) Study of physicochemical synthetic identity (structural and surface);
- Level 3) Evaluation of exposure related physicochemical properties (colloidal properties in exposure relevant media);
- Level 4) Evaluation of hazard related physicochemical properties (ions dissolution) and biological effects (in-vitro and in-vivo studies);
- Level 5) Performance evaluation, to verify unaltered product activity.

This procedure allowed to obtain three main results:

I. Development and validation of the modifications within a SbyD thinking.
II. Deep toxicological assessment for commercial available nanomaterial.
III. Gathering of (eco)toxicological data useful for future materials.

The activity strongly focused on the characterization of physicochemical intrinsic properties under laboratory condition and in the media typical of human and ecotoxicological tests. For studied CuO NPs a complete colloidal characterization in terms of Z potential, hydrodynamic diameter, ion dissolution and stability over time was performed for pristine material and for each proposed modifier. Particularly, a great effort was employed for the assessment of the CuO ion release in several media, developing a new electrochemical platform able to make in situ ion concentration measurements.

The main results provided a guidance for a justification of safer by molecular design strategies and their acceptance as technological alternatives/risk mitigation measures (TARMM) strategies in SUN Decision Support System (SUNDS).

Ongoing work is still in progress in order to improve the correlation between PCHEM properties and (ECO)-TOX effects, completely evaluate the performance of the proposed new material and evaluate its long-term, chronic, toxicity.

7.2 Parallel development

This project has been developed in collaboration with the European FP7 framework; the collected data supported the initiative to build a unified database to use in order to provide computational predictive models. Such models allow to estimates the behaviour of toxic materials, through appropriate simulations by in silico analysis and QSAR (quantitative structure-activity relationship). This effort will facilitate the evaluation of risk control strategies for nanomaterials proposals in the future.

To build reliable predictive models, large amounts of data on the behaviour of the considered material are required. Since the number of variables involved during the experiments influences the quality of these data, during this project other

characterization techniques have been examined. Electrochemical techniques for the determination of dissolved copper fraction (potentiometry and voltammetry) provided a fast and non-destructive characterization path: this permits to collect large sets of data relating to only one experimental condition, where different variables are not altered.

Recently showed a predictive nano-QSPR model developed to estimate Z-Potential for pure, spherical, metal oxide NPs after determination of the primary size [1]. After solubility has been identified as main activity responsible for the NPs toxicity, different techniques have been compared in order to analyse it and rapidly collect computational input for similar modelling prediction of adverse effects. Between the examined processes, innovative high throughput screening techniques were explored, starting collaborations with Metrohm, electrochemical equipment manufacturer. Initial results showed that cyclic voltammetry is well suited for the measurement “in situ” with eco-tox media, without amino acids. A technique for the determination in cell culture media has still to be found due to chelation interference. The final goals of the predictive modelling development are to reduce the time required for risk assessment for new materials, assisting in the introduction of SbyD alternatives and fully comprehend toxicity mechanisms while progressively extend the models to embrace different nanomaterials.

7.3 References

[1] A. Mikolajczyk, A. Gajewicz, B. Rasulev, N. Schaeublin, E. Maurer-Gardner, S. Hussain, J. Leszczynski e T. Puzyn, «Zeta Potential for Metal Oxide Nanoparticles: A Predictive Model Developed by a Nano-Quantitative Structure–Property Relationship Approach,» *Chemistry of Materials,* vol. 27, n. 7, pp. 2400-2407, 2015.